5-2018

# Gas-Phase Hydrogen-Deuterium Exchange and Fragmentation Studies of Tetrapeptides Containing Lysine and Its Homologs

AnnaTram Do

Gas-Phase Hydrogen-Deuterium Exchange and Fragmentation Studies of Tetrapeptides Containing Lysine and Its Homologs

A thesis submitted in partial fulfillment of the requirement
for the degree of Bachelor of Science in Chemistry from
The College of William and Mary

by

AnnaTram Ngoc Do

Accepted for Honors

John C. Poutsma, Director

Dr. Rachel E. O'Brien

Dr. Tyler K. Meldrum

Dr. Mark H. Forsyth

Williamsburg, VA
May 4, 2018

## Table of Contents

**Acknowledgements**

I would like to thank Dr. John C. Poutsma for the opportunity to do research. I am grateful for his mentorship and guidance throughout my honors project. I would like to thank my fellow Ionlab 2016-2018 lab members, especially Melanie Berger, Anwar Radwan, Danielle Long, Zach Smith, Amy Schienschang, for their help when needed, and for making my undergraduate research experience memorable. I would like to thank the W&M Charles Center for Honors Fellowship financial support to conduct summer research. Finally, special thanks to my friends and family, and committee board members, who had faith and supported me throughout this process

## List of Figures



## List of Tables

Abstract

Mass spectrometry- based proteomics is becoming a common method in proteomics. Peptides can be identified by automated database searches, and relative protein abundances can be obtained from the mass spectra. Understanding the fragmentation mechanisms may refine and provide additional "rules" that will increase the confidence in automated primary sequencing of peptides and eventually relate the information on gas-phase fragmentation patterns and energetics of dissociation to the gas-phase conformations of intact and fragment peptides and proteins; this will improve protein identification and profiling. Improvements are necessary for continual use of these quantitative approaches and bottom-up proteomics.

Lysine and its homologs, ornithine, DABA, and DAPA have been shown to affect fragmentation patterns based on their basicities. Lysine-analog containing tetrapeptides and their fragments were analyzed using hydrogen deuterium exchange (HDX) in a modified ESI-ion trap mass spectrometer. Fragments in this study were obtained using collision induced dissociation (CID). This study involved systematically varying the position of lysine and its homologs in the tetrapeptides, XAAA, AXAA, AAXA, and AAAX, where X is lysine or its homolog and A is alanine. Positional variance and systematic difference in side chain length affects the hydrogen deuterium exchange reaction. Results suggest that tetrapeptides containg short, basic side chains like Dapa, possess weak intramolecular bonds. Longer side residues have stronger intramolecular boning schemes in tetrapepetides. Results suggest that $b_n^+$ ions are either diketopiperazine or lactam structures. In addition, HDX was used to indirectly probe the structures of $XA^+$, $AX^+$, $AAX^+$ $b_n^+$ ions. Further investigations using IRMPD spectroscopy is necessary to identify b ion structures.

# Chapter 1: Introduction

## 1.1 Introduction to Proteomics

Cells are autonomous systems which are controlled by extremely complex genetic programs. The central dogma of molecular biology (Figure 1.1) is the explanation of the way in which the information is encoded, decoded, maintained, copied, and transmitted within the cell. Information usually flows in one direction from DNA to RNA to protein (central dogma), however there are special cases, in which this process is altered, which typically only occur in viruses. Transcription is the process by which pieces of information are copied from the DNA molecule to be encoded in the form of ribonucleic acid (RNA) molecules. Translation is the process by which most of the information copied from the DNA to RNA becomes codes for protein synthesis. Proteins are then transported to various areas of the cell to serve their function [1].

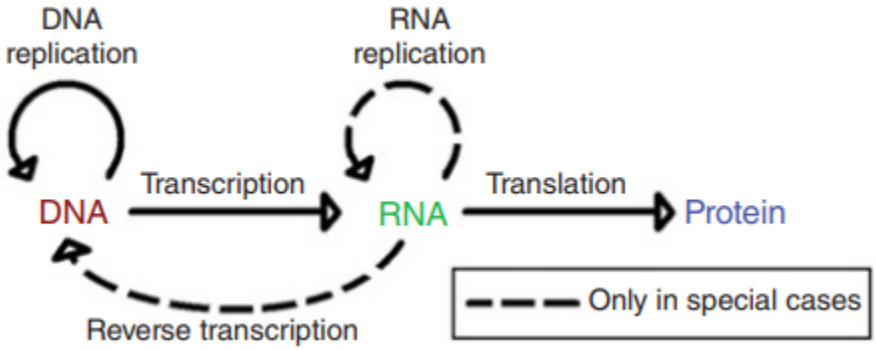


**Figure 2.1: Central Dogma of Molecular Biology. Adapted from [1].**

Figure 1.1 shows the basic flow of information, and is highly relevant in today's research in bioinformatics. In bioinformatics, analysis is dependent on generating and examining large datasets. Examples of datasets are microarray (gene expression) datasets and next-generation sequencing (NGS) datasets [1]. Vast numbers of DNA sequences exist in databases, however, merely having complete sequences of genomes is not sufficient to predict biological function [1-

2]. Genes and their protein complement or ‘proteome’ have no strict linear relationship, which is why proteomics remains as a multifaceted, rapidly developing and open-ended endeavor [1-3]. Proteomic studies focuses on the gene products, proteins, which are the active agents in cells. Proteins are responsible for metabolic and regulatory pathways necessary for a cell to live. Unfortunately, there can be modifications of the structure of the proteins that are not completely evident from the DNA sequence. Protein isoforms, and post-translational modification, such as glycosylation, phosphoryalation, and alkylation, are examples of these modifications [2]. Thus, to fully understand the proteome, the proteins themselves must be investigated.

### 1.2 Mass Spectrometry-Based Proteomics

Mass spectrometry has become a vital tool for identification and structure elucidation of proteins and peptide [2]. Mass spectrometry-based proteomic studies have identified possible internal and surface interactions in proteins, which elucidate possible folding and protein interactions [3-4]. Biological studies usually separate proteins using gel-electrophoresis techniques. However, an alternative strategy is to use liquid chromatography (LC) techniques such as high performance liquid chromatography (HPLC) or nanoHPLC to separate. Once proteins are separated, they can then be analyzed through top-down or bottom-up approaches. In top-down proteomics, the intact proteins are analyzed by mass spectrometry [2-4]. The top-down approach is limited by poor protein fractionation, mass spectrum resolution, and complications in fragmentation of large proteins. Although recent advances in Fourier transform ion cyclotron resonance (FT-ICR) and orbitrap mass analyzers have increased the feasibility of top down proteomics experiments through increased mass resolution and dynamic range, experimentation via these techniques are costly [5]. In addition, the molecular weight of proteins is not usually

sufficient for database identification, and some affordable mass spectrometers are unable to detect large molecular masses. The advantage of top-down proteomics is the ability to characterize post-translational modifications and conducting profiling proteomics experiments [4].

Alternatively, bottom-up mass spectrometry-based proteomics relies on digestion of gel-separated proteins into peptides by a sequence-specific protease, such as trypsin [4-5]. Peptides are easily eluted from HPLC columns and a small set of peptides from a protein provides adequate information for identification [5]. Peptide mapping is a bottom-up strategy, which involves analyzing the digested protein and obtaining peptide mass fingerprints (spectra). Peptide mapping is an important technique for investigating protein primary structures and determining surface-exposed sites or epitopes within proteins. It can be adapted to obtain internal protein sequences. Peptide mapping is a rapid method to identify the amino acid sequence of the target proteins. This method analyzes only the mass of the peptide, which is then compared to the theoretical peptide masses of known proteins, to speculate the identity and sequence of the target protein [4-6].

Proteomics has continued to gain a steady momentum with the development of new technologies and of new approaches. Currently, mass spectrometry-based methods and protein microarrays have become the most common technologies being used for the studying and identifying proteins, especially in the development of quantitative methods of protein profiling. There are two mass spectrometry-based approaches used for quantitative protein profiling. The most common and established method involves using two-dimensional electrophoresis to separate proteins, based on their isoelectric point and molecular mass, followed by staining and selection of differentially expressed proteins to be identified by mass spectrometry [2]. Recent

progress to this approach includes improvements in electrophoresis separation, and protein detection, and increased reproducibility of proteome patterns [3-4]. The alternative approach is the use of stable isotope tags to differentially label proteins from two different complex mixtures. In this method, proteins within a complex mixture are labeled isotopically then digested to yield labeled peptides [4].

In both of these quantitative approaches, the peptides are separated by liquid chromatography (LC) and analyzed by tandem mass spectrometry. Peptides are identified by automated database searches (such as SEQUEST), and relative protein abundances are obtained from the mass spectra [2-6]. Improvements to each of these steps are essential to protein identification and profiling, hence further investigations and improvements in protein separation, mass determination and quantification, peptide sequencing, and database searching is important to the continual use of these quantitative approaches [1, 4, 6]. In addition, as more full-length genes are represented in the database, the success rate of identification will increase further [2-6].

Paizs and Suhai (2004) explain that ion m/z (molecular mass of ion /charge of ion) and fragment ion abundance dimensions for general peptide entries of databases are difficult to generate [7]. Protonated peptides dissociate from different fragmentation pathways, and some peptides show selective and/or secondary fragmentation [8]. There are some amino acid residues that produce poor MS/MS spectrum. Given these challenges, existing sequencing programs and algorithms typically only use the m/z values of the most significant sequence ions, and do not use any fragment ion intensity-related data. In addition, gas-phase properties, interactions between amino acid side chain groups, and selective cleavages are often neglected sequencing programs and algorithms [5].

Providing additional "rules" can increase the confidence in automated primary sequencing of peptides and eventually relate the information on gas-phase fragmentation patterns and energetics of dissociation to the gas-phase conformations of intact and fragment peptides and proteins [6-8]. The rules of fragmentation can be explored from a “top-down” and bottom-up” approach. The first, a ‘top down’ strategy is a statistical approach based on systematic assessment of large databases containing tandem mass spectra of protonated peptides to derive fragmentation rules. Alternatively, the ‘bottom up’ chemical approach involves systematic investigation of the major fragmentation pathways of protonated peptides to increase our knowledge the chemistry behind the dissociation. Efficient peptide sequencing algorithms need to rely on understanding utilizing and refining fragmentation pathways and the inclusion of ion intensity relationships will improve protein identification using tandem mass spectrometry [8].

### 1.3 Tandem Mass Spectrometry

Mass spectrometry separates ions by their mass to charge (m/z) ratio. It can be used to identify and quantify compounds, to study thermodynamic properties, and to elucidate chemical structure. The apparatus used in this study was a modified quadrupole ion trap equipped with an electrospray ionization (ESI) source. ESI is a soft-ionization technique that is one of the most advantageous ionization source for studying biomolecules, as it can allow for ionization of intact biomolecules, unlike hard ionization techniques which leads to cleavage. ESI uses electrical energy to transfer ions from a solution into the gaseous phase before they are subjected to mass spectrometric analysis. Neutral compounds are converted to ionic form in solution by protonation [9-10].

The transfer of ionic species from solution into the gas phase starts with forming highly charged droplets with the same polarity as the needle voltage. The application of a nebulizing gas (nitrogen), enhances a higher sample flow rate [9]. The charged droplets, generated at the exit of the electrospray tip, pass down a pressure gradient and potential gradient toward the analyzer region of the mass spectrometer. Elevated ESI-source temperature and nitrogen drying gas continue to reduce the size of charged droplets by evaporation of the solvent, leading to an increase of surface charge density and a decrease of the droplet radius (increases sensitivity of m/z ratio). The final step of ESI occurs when the droplets obtain an electric field strength above a critical point and "Columbic" explosion occurs, at which it is kinetically and energetically possible for ions at the surface of the droplets to be ejected into the gaseous phase [9]. The emitted ions are sampled by a sampling skimmer cone and are then accelerated into the mass analyzer for analysis of molecular mass and measurement of ion intensity [9-10].

Following ESI, the ions enter the mass analyzer, which in this study was an ion trap. Ion traps are capable of performing tandem CID monitoring. An ion trap is composed of three hyperbolic electrodes: the ring electrode, the entrance end cap electrode, and the exit end cap electrode [9]. The electrodes form a cavity to trap and analyze ions. Ions travel through, enter, or leave through small holes in the center of both end caps. The ring electrode is located between the end cap electrodes. Ions produced from the source enter the trap through the entrance end cap electrode. Varying RF and AC potentials are applied to the ring electrode to produce a stable potential field that will trap ions in the device. During detection, the electrode system potential is altered to produce instabilities to eject the ion of desired m/z ratio. The ejected ions iare focused by an exit lens and detected by the ion detector system, such as an electron multiplier [9-10].

During MS/MS, the precursor/parent ion, is selected inside the trap and is allowed to undergo collision-induced dissociation with the background helium buffer gas at elevated lab-frame collision energies. After that, the product ions are ejected for detection. Alternatively, the product ions (peptide fragments) can be kept inside the trap, and another CID reaction can be initiated and this repeated CID reactions can continue for several iterations. (denoted as $MS^n$ in which n is the number of CID reactions) making it possible to examine further fragmentation [9].

## 1.4 Fragmentation

### *1.4.1 Mobile Proton Model*

Exploring fragmentation by mass spectrometry is essential to the bottom-up approach, as the mass spectra are dependent on how the peptides fragment in the mass spectrometer. Peptide fragmentation pathways in tandem mass spectrometry are studied to further understand the effects that different amino acid residues within the peptide sequences have on the fragmentation patterns [4-7]. When ionized by positive ion mode ESI, singly charged peptides are protonated at the most basic site within the peptide to produce a thermodynamically favored protonated species [44], which typically is the N-terminus of the peptide. However, basic amino acid residues such as lysine, arginine, or histidine have side chains that are more basic than their N-termini, hence protonation occurs on the side chain chain for peptides containing these residues. When activated, peptides are expected to show random cleavage along multiple sites in the peptide backbone as shown in Figure 1.3 [7]. Several residues can suppress these random cleavages and undergo selective cleavages that preferentially form specific product ions [7-8]. Further investigation on gas-phase fragmentation patterns and the energetics of dissociation can relate to the gas-phase conformations of intact peptides and proteins and can improve our

understanding of fragmentation “rules”. Further investigation of these additional "rules" provided by understanding the fragmentation mechanism will also increase the confidence in automated sequencing of peptides and proteins by tandem mass spectrometry [7-8, 11].

Dongre et al. (1996) have demonstrated that the mobile proton model leads to peptide dissociations that are a result of charge-directed cleavages initiated by intramolecular proton transfers. As seen in Figure 1.2, the most basic site is protonated, and upon activation, the proton can transfer to a number of possible sites on a peptide, prior to fragmentation, depending on energetic and bond orders [7-8]. Dongre et al (1996) suggests that the internal energy required for proton mobilization to occur is influenced by the difference between the energy of the most stable form and the protonated form generated after proton mobilization. The kinetics of this process can also be influenced by the time scale and instrument used. Dongre and coworkers analyzed this model on the time scale of a few microseconds [7-8].

`

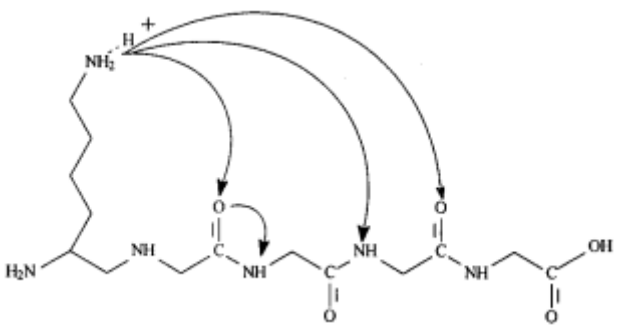

**Figure 1.2: Proton Mobile Model. Adapted from [8].**

According to Paizs and Suhai (2004), protonated peptides activated under low-energy collision conditions fragment mostly by charge-directed reactions, which involve migration of the added (“mobile”) proton and rearrangement. The internal energy of the ions increases upon collision and excitation allowing for the proton to migrate to other sites in the ion (proton

accepters such as the amide oxygens and nitrogens), as seen in Figure 1.2. Protonation near the amide bond it weakens the amide bond, and the carbon atom of the protonated amide group becomes a likely target of a nucleophilic attack of nearby electron-rich groups [45]. The fragmentation pattern depends on a number of parameters including the nature of the basicity of the amino acid residues, the length of the peptide, the excitation method, the time scale of the instrument, and the charge state of the ion (positive or negative) [7-8]. Under low-energy collision conditions, peptide precursor ions fragment along the backbone at the amide bonds. Fragment ions arising from the cleavage of this bond are known as b- and y-ions. Possible dissociation fragments are shown in Fig 1.3.

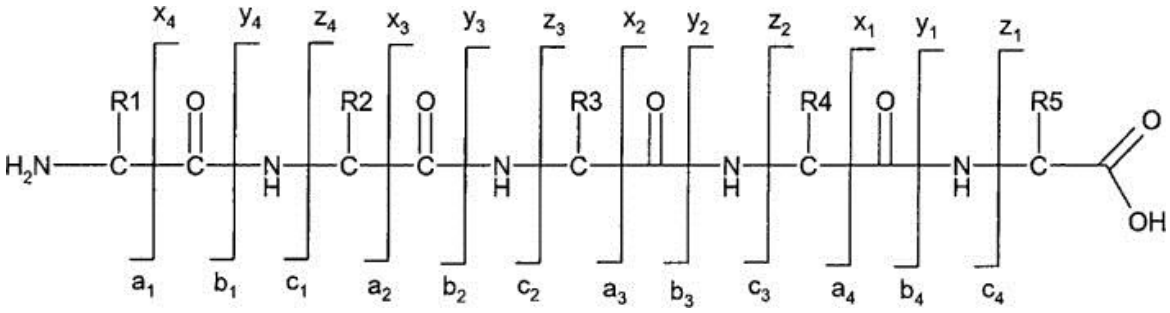


**Figure 1.3: Fragment Ions Resulting from CID. Adapted from [7]**

The "proton mobile model" is sufficient in explaining possible pre-dissociation reactions accessibility or inactivity of proton-transfer pathways which lead to reactive intermediates of ion fragmentation [7]. However, the probability of dissociation also depends on the energetic and kinetic accessibility of the reactive configurations and on the actual rate constants of the bond cleavages. Other pre-dissociation considerations include proton transfer reactions, transitions between isomers and tautomers, and *cis–trans* isomerization of amide bonds. Usually, the fragment with larger proton affinity will keep the added proton responsible for the charge-directed dissociation [7-8]. The formation of fragment ions of protonated peptides relies on

mechanistic, energetic, and kinetic aspects of the pre-dissociation, dissociation, and post-dissociation [7].

### *1.4.2 Formation of $b_2^+$ Fragments*

Under low-energy conditions, b- and y- ions form because the excited ions do not have enough energy to fragment on direct bond cleavage pathways. Therefore, the majority of ions of protonated peptides that are formed, undergo unspecified fragmentation pathways of either the amide oxygen attacking the neighboring amide carbon (oxazolone formation) [45], or the nitrogen of the N-terminal amino group attacking the carbon center of the protonated amide bond to induce dissociation (diketopiperazine formation), seen in Figures 1.4 and 1.5, respectively [7, 12].

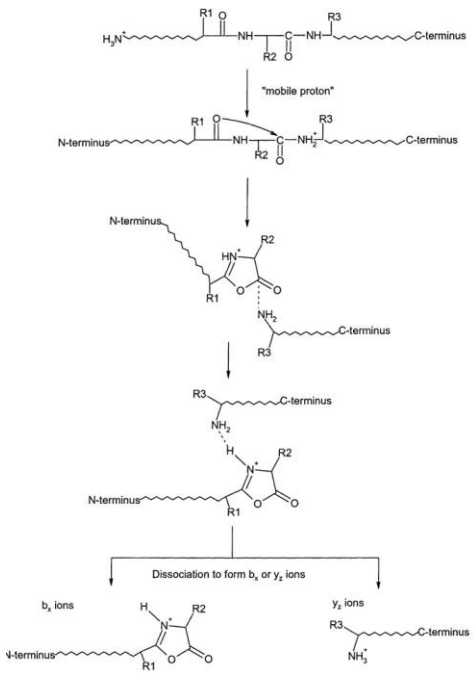


**Figure 1.4: Mobile Proton Mechanism of b ion oxazolone formation and y ion. The ion-neutral complex can dissociate and the proton can transfer to either the b or y ion. Adapted from [7]**

Infrared multiphoton dissociation (IRMPD) studies have experimentally shown that b ions will form the less stable oxazolone due to kinetic constraints [7, 45]. In addition, studies have demonstrated that $b_2^+$ ions that contain only aliphatic or simple aromatic residues are are almost exclusively oxazolone structures [7, 11-12, 13]

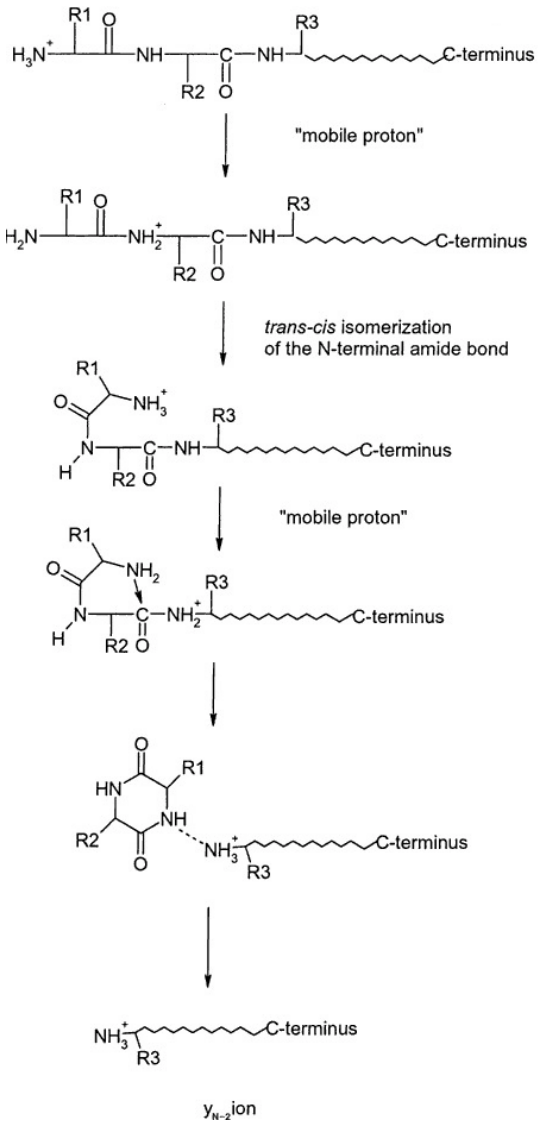


**Figure 1.5: Mobile Proton Mechanism of b ion diketopiperazine formation and y ion. The ion-neutral complexes can dissociate and the proton can transfer to either the b or y ion. Adapted from . Adapted from [7]**

The formation oxazolone or diketopiperazine b ions has been suggested to be dependent on the length of the peptide chain and the identities of the first three amino acid residues [7, 14]. Although diketopiperazine is the thermodynamically favored structure compared to oxazolone structure [14-15], there is a necessary *trans-cis* isomerization required in the precursor peptide prior to diketopiperazine formation. Studies have proposed that basic side-chain residues facilitate the formation of the diketopiperazine structure by providing a protonated nitrogen in a location that can allow for proton transfer or bridging to the nitrogen of the amide bond [7, 15-16].

IRMPD studies have also suggested that a mixture of both structures could be formed. Gucinski et al. (2012) showed that histidine residue systems had formed diketopiperazine, with the presence of some oxazolone structures. Using hydrogen deuterium exchange (HDX) and density functional theory (DFT) calculations, the authors suggest that histidine residues may inhibit complete *trans-cis* isomerization, allowing for the oxazolone pathway to still proceed [15]. Computational modeling has shown that intramolecular hydrogen bonding can stabilize oxazolone b ion structures [16]. In addition, for arginine, histidine, and lysine, additional cyclic lactam structures arising from attack of the side chain on the activated carbonyl group are possible and can be more stable than the oxazolone structures [17].

Figure 1.6 below shows a summary of the fragmentation pathways of interest to this study. The figure shows that based on the mobile proton model that the carbonyl is activated and that allows attack on the electropositive carbonyl. The attack from the adjacent carbonyl may result in forming an oxazolone. The attack from the N-terminus results in forming a diketopiperazine. The attack from the side chain results in a lactam formation.

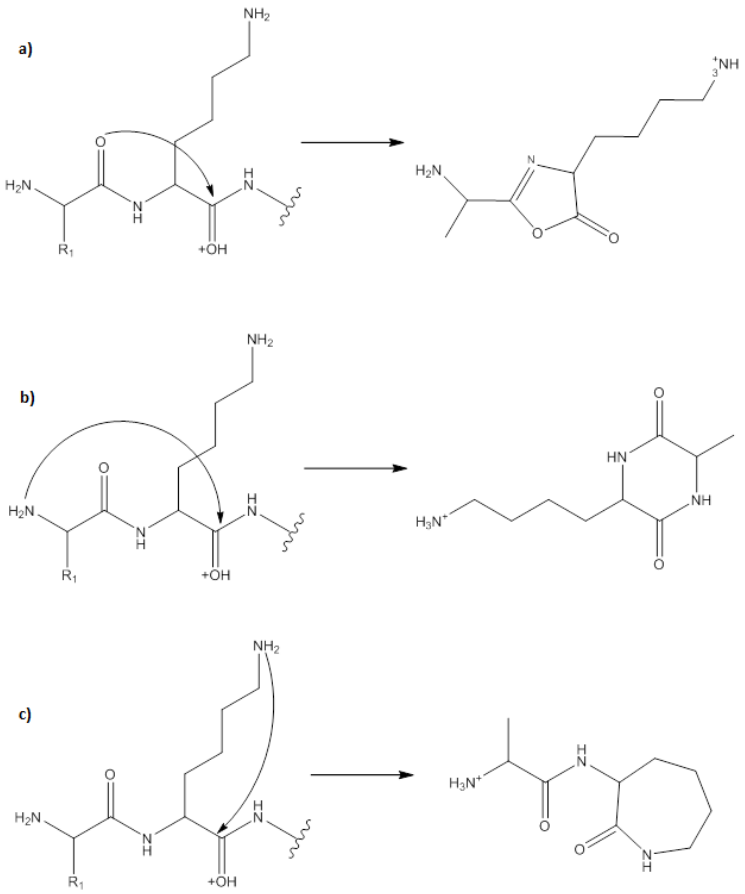


**Figure 1.6: Possible Fragmentation Mechanisms for Lysine. (a) Formation of oxazonlone (b) formation of diketoperazine (c) Formation of lactam**

*1.4.3 Selective $b_n^+$ Ion Formation and Cleavages*

Much interest is found with regards to how arginine and lysine produce unusual effects on the peptide that can result in formation of different fragments [3-6]. In accordance with mobile proton model, basic sites, such as the N-terminal amine, and basic side residues are commonly accepted to be the locations for excess protons in ions of low internal energy. Activation of the peptide ion allows the proton to move in order to inhabit different sites along the peptide backbone, protonation of the backbone amide leads to cleavage that produces b- and y-type ions, this is the most common cleavage observed for CID experiments. Depending on the

amino acid side chain, other selective cleavages may arise. For example, under specific conditions selective cleavages are observed at aspartic acid, proline, and histidine [5, 7, 12, 37].

The aspartic acid effect involves a proton being seized from the aspartic acid residue, which causes cyclization of the side chain. This cleaves C-terminal to the aspartic acid to produce a terminal succinic anhydride and a new primary amine [5, 7, 37]. This is known as a charge-remote fragmentation pathway as the proton is not necessary mobile or directly involved in cleavage. However, it is readily observed with a nearby arginine residue, which serves to take the proton away from aspartic acid [7, 37].

Alternatively, the proline effect involves a selective cleavage at the N-terminal to the proline due to the higher proton affinity (gas basicity) of the tertiary nitrogen, compared to its neighboring amide bonds. In this scenario, the ionizing proton is directly involved in the cleavage and is therefore said to be a charge-directed fragmentation pathway. Both of these cleavage phenomena have been found to dominate spectra under conditions favorable to the particular pathways [7, 19].

The histidine effect involves selective cleavage at the C-terminal side mediated by the nucleophilic attack by the protonated histidine side chain, and produces a unique bicyclic b ion fragment [5, 7]. Literature has also shown that histidine can initiate the aspartic acid effect. [20].

Ornithine is an amino acid that is nonproteogenic but is produced in nature via deguanidination of arginine and plays a role in the urea cycle [21]. It is expected that ornithine is more similar to lysine than arginine, based on the proton affinity of ornithine, and the side chain composition of which is one methylene group shorter than lysine [22]. However, ornithine exhibits a neighboring group effect, which leads to a selective cleavage at the C-terminal to the ornithine residue.  Furthermore, McGeen and McLuckey (2013) have reported that the ornithine

effect is appears to dominate compared with the aspartic acid and proline effects using a peptide in which all three processes can compete [21]. In addition, ornithine can generate b ions that are neither oxazolone or diketopiperazine, but rather a lactam. The cyclized ion produced by a nucleophilic attack of the carbonyl carbon by ornithine's side chain to form a six-membered lactam [21-22]. It is necessary to study these selective cleavages as the dominance of these cleavages may lead to a loss of fragmentation information because other fragment peaks may be of very low intensity or not present [5, 7].

### *1.4.4 Molecules and Fragmentation Mechanisms of Interest*

Arginine and lysine have high proton affinities and the side chains of these amino acid residues compete effectively for the mobile proton [7, 21-22]. Studies have shown that it is possible that these basic side residues exert a localization effect on the proton; making the proton less mobile, and that the effect reduces backbone fragmentations for singly protonated arginine-containing peptides [12, 21].

In addition**,** lysine has a number of possible fragmentation pathways, hence lysine (K) and its homologs ornithine (O), 2,4-diaminobutanoic acid (Daba) and 2,3-diaminopropanoic acid (Dapa) are the amino acid residues studied in this tetrapeptide fragmentation study. These amino acids all differ by the number of carbons in their respective side chains [5, 22]. Lysine is the amino acid residue of this set that is biologically encoded for in humans, and although its homologs are not coded for, they may exist biologically [5, 21]. Studying the fragmentation patterns of peptides containing lysine homologs may provide insight into the fragmentation mechanisms of lysine containing peptides.

Using the extended kinetic method, the proton affinities of lysine and its homologs were previously determined to be 1004.2 ± 8.0, 1001.1 ± 6.6 , 975.8 ± 7.3, and 950.2 ± 7.1 kJ/mol for lysine, ornithine, Daba, and Dapa, respectively [22]. The differing proton affinities may affect the fragmentation patterns of peptides containing these residues [23]. The characteristics of the homologs fragmentation patterns can provide insights into gas-phase peptide fragmentation and the characteristics of lysine-containing peptide fragmentation. Studying the mechanisms of peptide fragmentation containing these species can improve peptide sequencing databases and the continuity of studying bottom up proteomics using mass spectrometry [5].

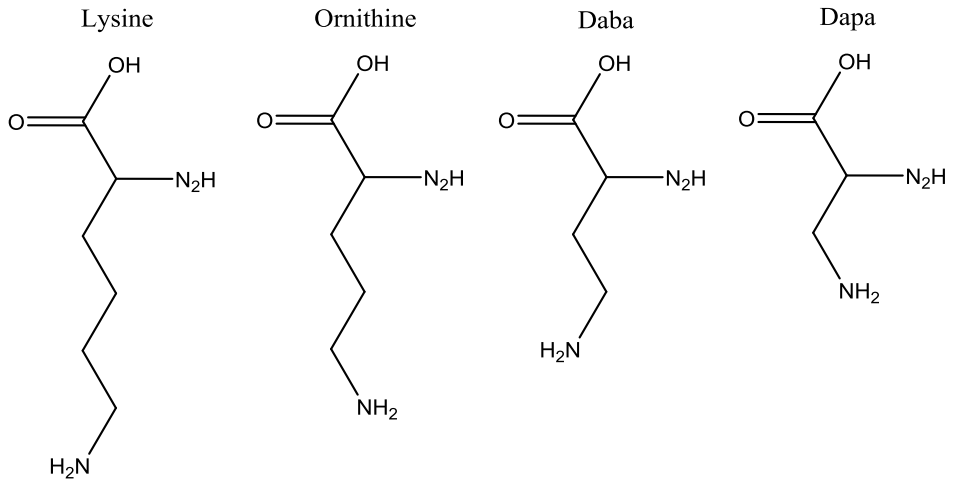


**Figure 1.7: Neutral Structures of Lysine, Ornithine, Daba, and Dapa**

Lysine and its homologs have similar functional groups that vary in side chain length. This systematic difference in side chain length was shown to affect the hydrogen deuterium exchange or the fragmentation mechanism as the there is a change in proton affinity (PA) of lysine PA> ornithine PA> Daba PA > Dapa PA [5, 22]. Literature has suggested that positional variance also affects gas-phase basicity, and knowing the identity of the first three residues is essential to fragmentation mechanism [7, 14, 22, 24]. Hence, this study involved systematically

varying the position of lysine and its homologs in the tetrapeptides, XAAA, AXAA, AAXA, and AAAX, where X is lysine or its homolog and A is alanine, as seen in Figure 1.7. Alanine was used as a filler amino acid, as it is a small, nonpolar, and cost effective amino acid [5].

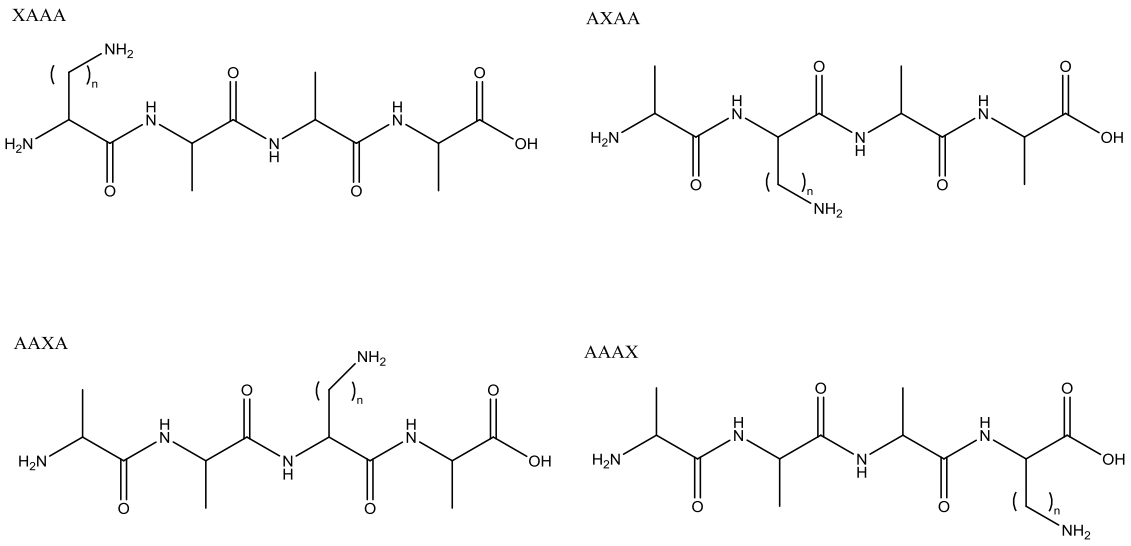


**Figure 1.8: Varying Positions in Tetrapeptides (n=1 for Dapa, n=2 for Dapa, n=3 for Onithine and n=4 for Lysine)**

Currently, our research lab is focused on identifying protein groups through using databases such as SEQUEST. Current work in our group uses the bottom up approach ("peptide-mapping" approach). In addition, previous fragmentation studies have been completed using lysine- containing tetrapeptides [5]. This study will further explore the structure of the tetrapeptides and their and b ion fragments. The aim of this study is to indirectly determine the effects of systematically varying the length of the side chain and the position of the residue in the peptide on the structure and intramolecular bonding schemes of these peptides using gas-phase hydrogen deuterium exchange. In particular, our group attempts to clarify if ornithine and lysine effects are applicable in tetrapeptides containing Daba and Dapa. In addition, this study serves to complement infrared multiphoton dissociation spectroscopy and density functional theory calculations on these species.

## 1.5 Hydrogen Deuterium Exchange (HDX) Mechanism

Hydrogen/Deuterium Exchange (HDX) is a chemical reaction where deuterium atom replaces covalently bonded hydrogen. The mass of deuterium is twice the mass of hydrogen, therefore the molecular mass increases as the peptide is increasingly deuterated. Mass spectrometry methods can detect the incorporation of deuterium based on the increase in mass. HDX studies have contributed to understanding interactions and mechanisms between amino acids. The mechanism of exchange varies depending on the interaction of the biomolecule with the deuterium donor, the structure of the reaction, and mechanism of isotopic exchange [25]. A factor that may affect HDX is the proximity of charge site to potential exchange site; for example, if exchange is seen, this suggests that the two heteroatoms are nearby each other, whereas, if exchange is not seen, then heteroatoms are not within distance of each other. Another factor affecting HDX is if the intramolecular interaction of the labile hydrogen atoms may be involved in a strong intramolecular bond. Thus, H/D exchange can provide indirect evidence of intramolecular bonding schemes [5, 7, 46]. Other factors affecting HDX frequency of collisions between deuterium and the ion, and energetics of ion-molecule complexation [46].

Campbell et al. (1995) conducted a study of protonated glycine oligomers with four deuterated alcohols: $D_2O$, $CD_3OD$, $CD_3CDO_2D$, and $ND_3$. Reaction kinetics are dependent on properties of exchange reagents. Their study demonstrated that increasing gas-phase basicity increases the rate and extent of hydrogen-deuterium exchange of the glycine oligomers. Hydrogen-deuterium exchange is dependent on the proton affinity difference between the hydrogen on the analyte and deuterating agent [25].

Campbell et al. (1995) proposed five mechanisms by which H/D exchange occurs for glycine oligomers, which can be seen in Figure 1.8 [25]. They propose that glycine oligomers

and deuterated bases such as $ND_3$, interact through an onium ion mechanism. The onium ion mechanism involves a proton transfer from the N-terminus followed by solvation of onium (ammonium) ion. The relay mechanism involves a proton transfer, by which a proton is transferred from the site of protonation onto the deuterated base, and concurrently, the deuterium atom is transferred to a slightly less basic site on the molecule. Deuterated bases that have low proton affinity, such as $D_2O$ or $CD_3OD$, undergo the relay mechanism [22, 25]. The salt bridge mechanism involves a proton transfer from the C-terminus to the deuterated base to form an ion pair that is stabilized by a nearby charge center. This mechanism was proposed for the exchange that occurs at C-terminus of betaine and glycine oligomers. Salt bridge formation is favorable for higher proton affinity agents. An alternative mechanism proposed for less basic reagents and relatively slow exchange for the C-terminus was the multicenter flip-flop mechanism. The tautomer mechanism involves a proton transfer from N-terminus to amide carbonyl and the transfer of amide proton to the deuterated base, and is highly favorable for exchange with $ND_3$ [25].

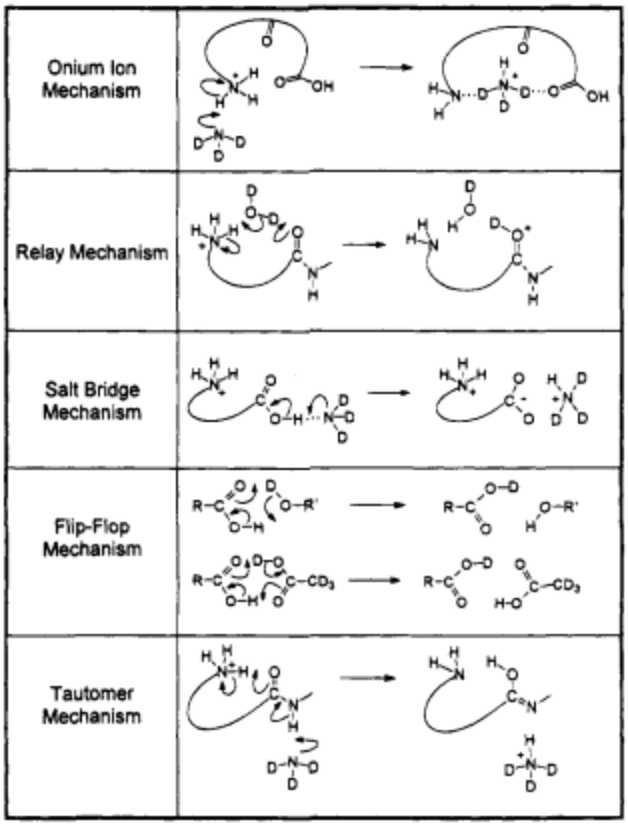


**Figure 1.9: Proposed hydrogen-deuterium exchange mechanisms for the glycine oligomers with reagent bases. Adapted from [25]**

Knowing which mechanism occurs depending on deuterium donor is essential in predicting the structure of different amino acids. In this study, the peptide was reacted with $D_2O$, which suggests that the exchange between $D_2O$ and the lysine side chain probably occurs through the relay mechanism, provided that there is a heteroatom nearby. The relay mechanism of exchange can be seen in Figure 1.9. Studies have shown that there is a relationship between the gas phase basicity and HDX behavior [22, 25-26, 46]. In addition, exchange through the relay mechanism occurs more willingly when the gas phase basicities of the locations on the ion are similar [25-26, 37-38, 46]. The relay mechanism is charge-directed, exchange is facilitated by two groups of similar basicity and are relatively close to each other (N-terminus and side residue) can be bridged by hydrogen bonding to $D_2O$ to form a stable ion-molecule complex

[46]. Subsequently, the N-terminal amine group is able to incorporate the deuterium atom from the $D_2O$ [17, 25-26, 38]. The relay mechanism is dependent on the availability of the hydrogens on the two basic sites for the deuterating agent to interact with. Another possible mechanism of exchange for low proton affinity deuterants such as $D_2O$ is exchange at the C-terminus through the flip flop mechanism as seen in figure 1.8,. The flip-flop mechanism involves direct interaction between $D_2O$ and labile hydrogen. As seen in Figure 1.8, $D_2O$ can form a pseudo-ring structure by attraction of partially charged participants allowing for exchange to occur [46]. Exchange will be slower at the C-terminus as this mechanism is independent of the charge site [25].

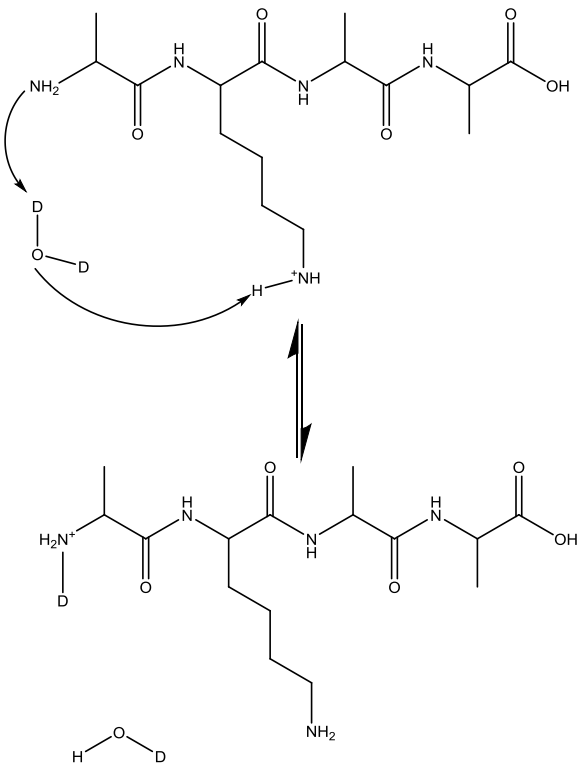


**Figure 1.10: Schematic of HDX relay mechanism involving $D_2O$ interacting with AKAA tetrapepetide. Exchange requires bridging of the deuterating reagent with two basic sites on the molecule in order for deuterium incorporation to occur.**

# Chapter 2: Experimental Methods

## 2.1 Peptide Synthesis

Peptides were synthesized from C-terminus to the N-terminus using a standard solid phase synthesis method [27]. In this method, the C – terminal amino acid is attached to a resin, usually an insoluble polyethylene bead. In this study, a Wang resin (4-hydroxymethylphenoxy) was used for synthesis. Peptide synthesis was conducting using disposable 3mL polypropylene syringes (reaction vessel) with a sealed in fritted disc. All steps of the peptide synthesis was induced with mechanical agitation of the syringe using an automated shaker. The fritted disc allowed the insoluble resin beads to stay in the tube while solutions used to de-protect and couple to the beads could be pumped out of the syringe. Solutions used in the coupling process of peptide synthesis included dimethylformamide (DMF), dichloromethane (DCM), piperidine, 2-(6-Chloro-1H-benzotriazole-1-yl)-1,1,3,3-tetramethylaminium hexafluorophosphate (HCTU) and N,N-diisopropylethylamine (DIEA). For all reaction steps, the amount of solvent added into the reaction vessel was enough to submerge all reactants in the reaction vessel in the solution, not necessarily using a consistent amount of solution or filling the syringe completely. Solution wastes were collected in a glass beaker during synthesis, which was later properly disposed of [5, 27].

The first step of peptide synthesis is swelling the resin, this is a necessary step because resin beads that are not well swollen in solvents can result in poor reaction site accessibility to the amino acids and diminished reaction and coupling rates [28]. In this study, the resin was swelled in 50:50 DCM:DMF. The amount of solvent mixture added is added until all the resin was covered. Following the swelling of the resin, the subsequent amino acids were added. These additional amino acids are protected on the amine side with fluorenylmethyloxycarbonyl (Fmoc),

whereas their carboxyl end are not protected. The protection group on the amine group is necessary to prevent unwanted reactions from occurring before coupling the following amino acid. Amino acid coupling takes several steps which can be described as the following: wash, de-protection of the residue on the resin, wash, coupling, and wash. After the coupling is completed, the peptide is cleaved off the Wang resin and precipitated with diethyl ether, and centrifuged into a solid. A generalized approach to peptide synthesis is seen below in Figure 2.1, which comments on the main steps (without mentioning the washing steps) [5, 27].

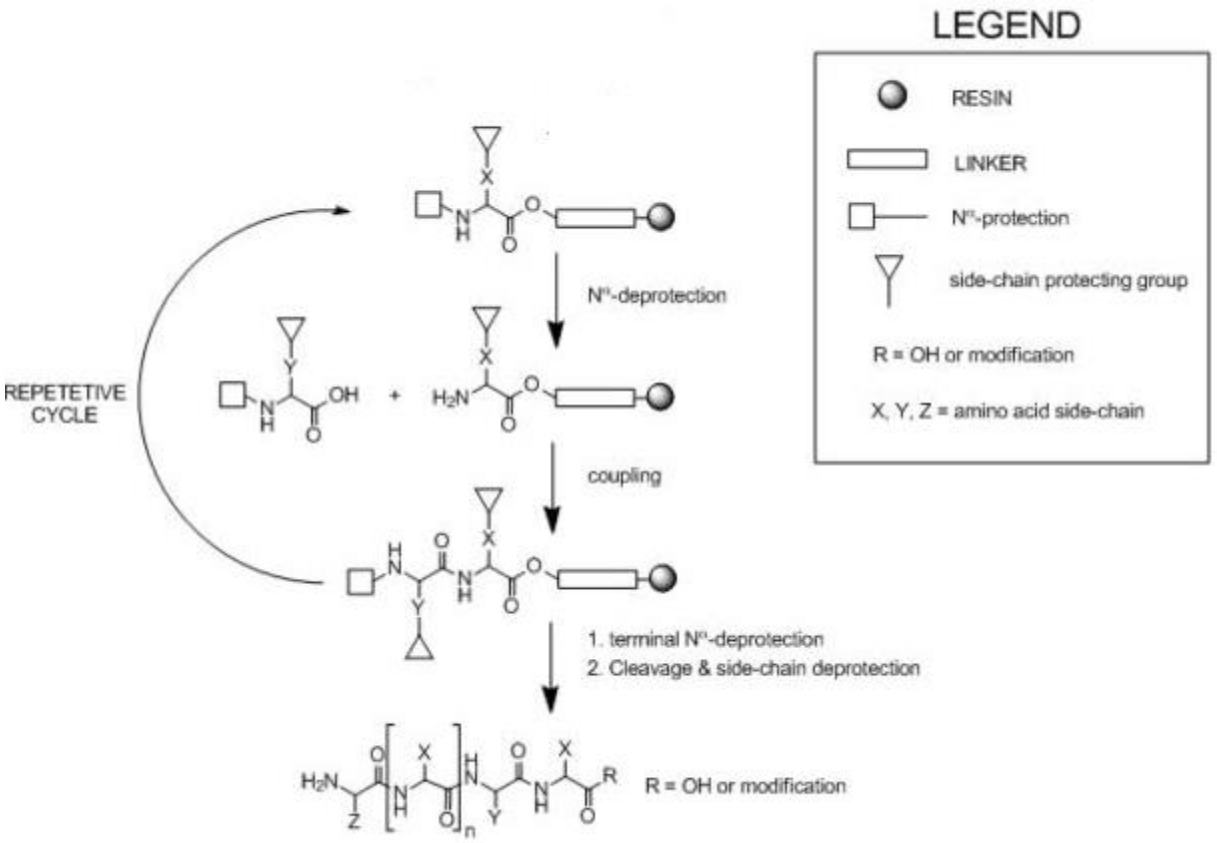


**Figure 2.1: Generalized approach to solid-phase peptide synthesis. Adapted from [27]**

The washing step consists of rinsing the resin with dimethylformamide (DMF) in the reaction vessel for 1 min; the DMF solution was pumped out. This washing step was done twice

to increase the purity of the final peptide, and wash away undesirable side-products before moving on to further coupling steps, and to increase yield [5, 29-30].

The de-protection step starts by removing the Fmoc from the N-terminus with piperidine. This step is essential to create a free N-terminus amine in necessary to react with the C-terminus carboxylic acid of the subsequent amino acid. This step consists of rinsing with DMF for 1 min, followed by one 5 minute and one 30 minute reaction step with 20:80 piperidine:DMF. The Fmoc group becomes labile and is deprotected using a solution of 20% piperidine in DMF [29]. The fluorene ring is deprotonated, which generates the aromatic cyclopentadiene intermediate, and eliminates to form dibenzofulvene. Dibenzofulvene then attached to the piperidine, which frees the N-terminus for the coupling reaction. The mechanism is seen in Figure 2.2 [5, 29, 31].

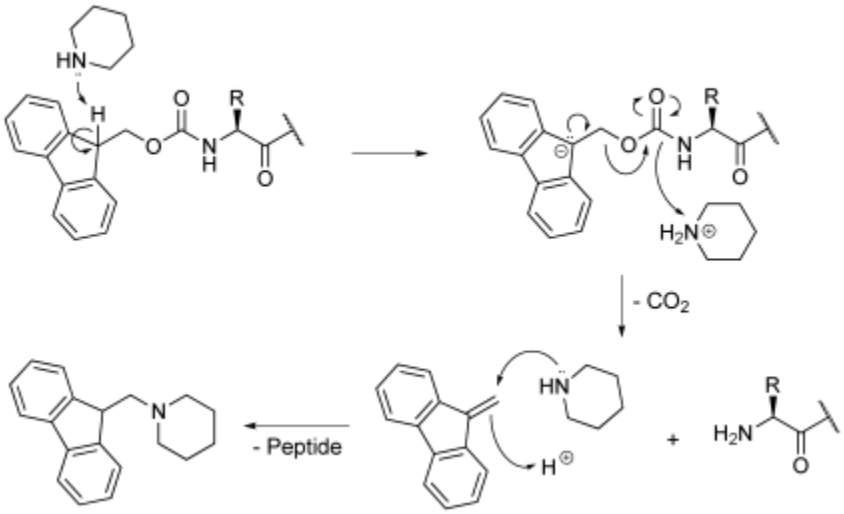


**Figure 2.2: Removal of Fmoc with Piperidine. Adapted from [31]**

Following de-protection, the piperidine solution is rinsed out, followed by two one-minute washes with DMF, then four one-minute washes with DCM. The DMF removes the residual piperidine, and DCM dries out the beads for the following step, coupling. The coupling step involves the addition of the next amino acid from the C-terminus. Two one-minute washes with DMF were added to the dried resin. Afterwards, the subsequent amino acid, DMF, and the

coupling reagents, HCTU and DIEA, were reacted for one hour. This coupling solution consisting of 2 molar equivalent amount of amino acid and HCTU, and a 4 molar equivalent amount of DIEA, was placed in the synthesis vessel with some DMF [5]. Amide bonds are typically synthesized from a nucleophilic attack on the carboxyl from the amine; however, the unification of the two functional groups is not spontaneous at room temperature. Therefore, the coupling agents were necessary to first activate the carboxylic acid of the amino acid, a process that converts the –OH of the acid into a good leaving group, and allowing the nucleophilic attack from the amine. Initially the amino acid will attack HCTU. DIEA will attack the carbonyl, and displace HTCU. DIEA reacts with the amino acid to form an active ester which enhances the reactivity and encourages nucleophilic attack from the amine [29-32]. Following the coupling, the unwanted solutions are pumped out followed by the washing step. The resin was washed with DMF for 1 min, this was done six times. This de-protection and coupling steps are repeated until all the amino acids desired in the peptide chain are added [5].

Following the addition of all necessary amino acids, a cleaving step involves removing the C-terminal amino acid from the beaded (Wang) resin. Fmoc protects the amine group to prevent undesired reactions during synthesis, however it is removed before the de-coupling step. Lysine and its homologs have amine side chains, and in order to make sure there were no reactions with the amine groups on these side chains, they are protected by using protecting groups like tert-butyloxycarbonyl (Boc) and 2,2,4,6,7-pentamethyldihydrobenzofuran-5-sulfonyl (Pbf). These protecting groups are removed at this cleaving step [5].

Prior to cleavage, there is a swelling in 50:50 DCM:DMF for 30 minutes, followed by a one minute wash. This is followed by a de-protection step to remove the Fmoc group on the last amino acid added. This step consists of rinsing with DMF for 1 min, followed by one 5 minute

and one 30 minute rinsing with 20:80 piperidine:DMF. Then 2 steps of 1 minute DMF wash. Afterwards, there are four 1 minute rinses with DCM, to completely dry the resin. Then 10mL of cleavage solution (95% trifluoroacetic acid (TFA), 2.5% deionized water, and 2.5% triisopropyl silane) was reacted with the resin for 2 hours [5] . Trifluoroacetic acid (TFA) is the cleavage reagent. The lone pairs on the amine on the amino acid will attack TFA to remove protection group or Wang resin, and this generates a highly reactive cationic species that can react with electron-rich functional groups on the amino acids and therefore modify the desired peptide (i.e. form secondary structures, hence, triisopropyl silane, a nucleophilic reagent, acts as a scavenger and quenches the ions that are formed [29-32]. No purification or chromatography was conducted in this study as the main concern of peptide synthesis in this study was the order of addition of amino acids. Thorough washing and drying steps allowed for the intended successive order of additional amino acids to be synthesize and avoid improper addition [5].

## 2.2 HDX-MS

### *2.2.1 Sample Preparation and Mass Analyzer Parameters*

Peptides were dissolved to in 50:50 MeOH:$H_2O$ with 1% formic acid solution. Solutions were further diluted to about $1x10^{-4}$ M. HDX is relatively slow process, therefore an instrument that is capable of trapping ions over long periods of time while they are undergoing collisions with $D_2O$ is necessary, a suitable instrument is the ion trap. H/D exchange of the tetrapeptides was carried out in a modified Thermo LCQ-DECA quadrupole ion trap mass spectrometer with an electrospray ionization source [5, 33].

. The H/D exchange reaction is affected by He/$D_2O$ pressure, which is adjusted for at the ion gauge by varying the flow of helium via a microneedle valve, and was usually kept between

1.9 -2.0 x $10^{-5}$ torr. H/D exchange in this study is also dependent on ratio of He/$D_2O$. The ion trap was modified to allow $D_2O$ to be leaked in with the helium line of the mass spectrometer. The sample was introduced into the mass spectrometer using a 500 µL Hamilton syringe at varying flow rates. After sample introduction, LCQ TuneTM software was used to optimize parameters prior to analyzing the protonated tetrapeptide of interest. This tuning program changes the voltages applied to the source and the offset voltages of the focusing lenses to attain the highest possible ion count of the specified m/z ratio [33].

In this study we used tandem mass spectrometry to monitor the hydrogen-deuterium reaction. The parent mass (tetrapeptide m/z) was isolated, reacted with $D_2O$, and reaction product ions were analyzed by the detector. When looking at hydrogen-deuterium exchange reaction, the collision energy was reduced to zero (0% NCE). $D_2O$ reagent was leaked into the helium line of the mass spectrometer at flow rates ranging from 200 to 400 µl/hr using an automated syringe pump when analyzing tetrapepetides. $D_2O$ was allowed to equilibrate for one hour in order to fill the ion trap before any data was collected. For H/D exchange of tetrapeptides, all masses were observed with an isolation width of 12m/z to observe all possible exchanges. The activation q-value was set to 0.250 for all masses. For this study the time scale for HDX in this study was ranged from ms to seconds. Activation times (which are proportional to reaction time) were set at 100, 1000, 5000, 10000, 5000+10000, 10000+10000, 10000+5000, 7500, 2500, 500, respectively. Spectra at activation time 10000 and lower are obtained using isolated in MS/MS zoom scan mode, and were collected with 3 averaged scans. However, LCQ TuneTM software limits the stage time to 10000 ms, hence observing exchange beyond 10000 ms requires additional set of parameters, and are viewed as $MS^3$ spectra and require 4 averaged scans [33-

34]. Data was taken at 5000+10000 ms and 10000+5000 ms were obtained to monitor for any latency in switch to $MS^3$ mode.

HDX studies of selected $b_n^+$ fragment ions from these tetrapeptides were conducted at same reactions times, number of scans and isolation widths but a lower $D_2O$ rate of 10-50μL/hr. Parent ion masses of the tetrapeptides were selected using the ion trap with an isolation width of 1-4 m/z. MS/MS was conducted in the ion trap using CID with helium as the collision gas to obtain tetrapeptide fragment ion mass spectra. CID activation of parent ion occurred at 20-85% normalized collision energy (NCE) and was optimized in order to maximize $b_n^+$ ion intensity.

*2.2.2 Generating Kinetic Plots*

Kinetic plots were generated by monitoring the disappearance of reactants and appearance of products ion intensities over time. Calculations of rate constants of the peptides were calculated using relative pseudo-first order rate coefficients [35]. Second order equations are quite difficult to manipulate, where as in a pseudo-first order reactions are more easily manipulated. A significantly high relatively constant concentration of $D_2O$ was used, while the other reactant, the tetrapeptide ion, has a low concentration. Reaction depletes the $D_2O$ concentration by only a small amount, therefore it is treated as a constant. Under this assumption, the reaction rate constant can be multiplied by the constant concentration of $D_2O$ to form a new rate constant (k') that will be used in the new rate equation, and treated as a first order reaction.

The kinetics of HDX in this study are as seen in the equations below for incorporation of one deuterium atom (not accounting for back exchange):

$$D_0 + D_2O \rightarrow D_1 + HOD$$

According to second order reaction the disappearance of $D_0$ over time is:

$$\frac{-d[D_o]}{dt} = k\,[D_0][D_2O]$$

The integrated form is:

$$kt = \frac{1}{[D_2O]_0 - [D_0]_0} \ln \frac{[D_2O][D_0]_0}{[D_2O]_0[D_0]}$$

Second order equations are difficult to manipulate, hence we used a high and constant concentration of $D_2O$, therefore assuming relative no change in $D_2O$ concentration, or ion abundance, over time:

$[D_2O] >> [D_0]_0$, then $[D_2O]_0 \approx [D_2O]$

$$kt = \frac{1}{[D_2O]_0 - [D_0]_0} \ln \frac{[D_2O][D_0]_0}{[D_2O]_0[D_0]} \approx \frac{1}{[D_2O]} \ln \frac{[D_0]_0}{[D_0]}$$

$$kt \approx \frac{1}{[D_2O]} \ln \frac{[D_0]_0}{[D_0]}$$

$$[D_0] = [D_0]_0 e^{[D_2O]kt}$$

$$[D_0] = [D_0]_0 e^{k't}$$

The integrated form has now become similar to a fist order reaction integrated form: Since $k' = k[D_2O]$, we assume pseudo-first order rate is:

$$\frac{-d[D_o]}{dt} = k'[D_0]$$

And that the reaction of the incorporation of one deuterium assumed in this study is:

$$D_0 \xrightarrow{k'} D_1$$

(Note: $[D_0]_0$ is the initial concentration of $D_0$. $[D_2O]_0$ is the initial concentration of $D_2O$, k' is the pseudo-1st-order reaction rate constant (which will be experimentally-obtained relative rate constant), k is the second order reaction rate constant (absolute rate constant), and $[D_0]$ is the concentration of $D_0$ at time t.):

Betaine is a molecule with only one exchangeable hydrogen of a known rate coefficient of $1x10^{-12}$ $cm^3$ $molecules^{-1}$ $s^{-1}$ [36]. This value, along with an experimentally-obtained relative rate constant ($k'$) was used to find the concentration of $D_2O$ inside the trap on each day that data was collected. Absolute rate coefficients were obtained using KinFit program in Microsoft Excel [35, 36]. Relative rates of HDX for in this study ranged from $10^{-11}$-$10^{-13}$ $cm^3$ $molecules^{-1}$ $s^{-1}$.

Qualbrowser was the software used to view raw data files of spectra obtained from LCQTuneTM. Average ion intensities for masses at each reaction time were exported into Excel and normalized at each activation time to account for differences in total ion signal. Normalized intensities vs time were plotted using a set of ordinary differential equations using the Kinfit kinetic fitting program [33, 35]. This program provided relative rate coefficients for each observed exchange. Two sets of equations were used to look at relative exchange, simple equations and back exchange equations.

Simple equations assume that exchange involves only the incorporation of deuterium as seen below:

$$D_0 \overset{k_1}{\rightarrow} D_1 \overset{k_2}{\rightarrow} D_2 \overset{k_3}{\rightarrow} D_3 \overset{k_4}{\rightarrow} D_4$$

The simple equations are shown below for 4 exchanges. $D_0$ through $D_4$ represents relative ion abundances, and $k_1$ through $k_4$ are the rate coefficients for each exchange [33]. Ydot(1) represents the change in the concentration of $D_0$ over time, K(1) is the rate coefficient $k_1$, and Y(1) is the population of $D_0$.

$$Ydot(1) = - K(1) * Y(1)$$

$$Ydot(2) = - K(2) * Y(2) + K(1) * Y(1)$$

$$Ydot(3) = - K(3) * Y(3) + K(2) * Y(2)$$

$$Ydot(4) = - K(4) * Y(4) + K(3) * Y(3)$$

$$Ydot(5) = + K(4) * Y(4)$$

The simple equations do not account for the possibility of back exchange, which is when the deuterium is replaced by a hydrogen at a site that has already undergone exchange. Whereas, the back exchange differential equations do. Possible back exchanges can be seen in the equilibrium below:

$$D_0 \underset{k_8}{\overset{k_1}{\rightleftarrows}} D_1 \underset{k_7}{\overset{k_2}{\rightleftarrows}} D_2 \underset{k_6}{\overset{k_3}{\rightleftarrows}} D_3 \underset{k_5}{\overset{k_4}{\rightleftarrows}} D_4$$

The set of equation that incorporates back exchange used for the above reactions are seen below:

$$Ydot(1) = K(8) * Y(2) - K(1) * Y(1)$$

$$Ydot(2) = K(1) * Y(1) + K(7) * Y(3) - K(2) * Y(2) - K(8) * Y(2)$$

$$Ydot(3) = K(2) * Y(2) + K(6) * Y(4) - K(3) * Y(3) - K(7) * Y(3)$$

$$Ydot(4) = K(3) * Y(3) + K(5) * Y(5) - K(4) * Y(4) - K(6) * Y(4)$$

$$Ydot(5) = K(4) * Y(4) - K(5) * Y(5)$$

It was determined that the isotope peaks had a relatively small impact on results, but that back exchange was significant, especially at longer reaction times. The back exchange equations were applied to all the tetrapeptides to determine the rate coefficients. The rate coefficients obtained from Kinfit are relative rate coefficients, and to determine absolute rate coefficients of the analyte tetrapepetides, relative rate values were divided by the concentration of $D_2O$ in the trap to obtain absolute rate constants [33, 35-36].

## Chapter 3: Results

The HDX spectra of the 16 synthesized tetrapeptides at 10000+10000ms are presented below. For ions, 10000+10000ms, is considered to be a very long reaction time, and if peak has not been seen at this reaction time, we consider it too slow to be measured under our reaction conditions. Kinetic plots show the ion intensities that correlate with increasing incorporation of deuterium over time. Most spectra were obtained at $D_2O$ flow rate of 200µL/hr, unless mentioned otherwise. Major product ion peaks have been identified and labeled on the spectra. Kinetic plots are provided in the Appendix. The mass spectrum is a graphical display of the relative abundance of ion signals versus the m/z ratios. The highest signal is taken as 100% abundance and all the other signals are expressed as a percentage of this.

### 3.1 X-Alanine-Alanine-Alanine

*3.1.1 KAAA*

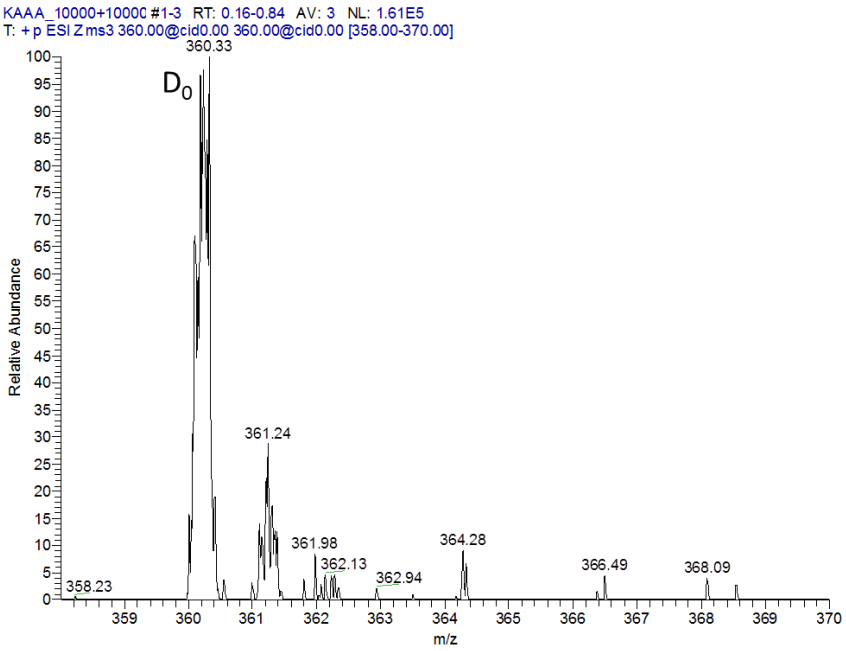

The HDX spectrum for KAAA shows that KAAA (M+H = 360) is present. There is no exchange seen in this plot. The kinetic plot (in Appendix) similarly supports that the ion abundances have not changes over (reaction) time. There is a relatively small peak at m/z= 361, which is representative of presence of $^{13}C$ rather than deuterium incorporation. $^{13}C$ makes up 1.11% of all carbon atoms [22]. The peak is relatively high in this spectra due to high ion abundance of KAAA.

*3.1.2 OAAA*

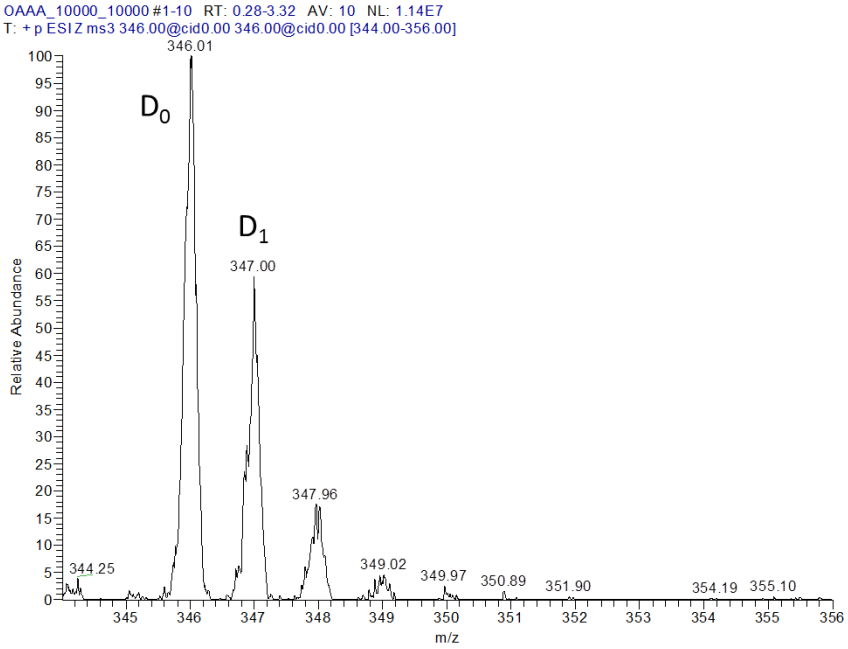


The HDX spectrum for OAAA shows that OAAA (M+H = 346) is present at a high ion abundance. There is one slow exchange indicated by this data at m/z=347. The kinetic plot (in Appendix) similarly supports that there is one extremely slow exchangefor OAAA. This one labile hydrogen may be located on the C-terminus of OAAA, and therefore exchange would be expected to occur through the flip-flop mechanism. There is a relatively small peak at m/z= 348, which is from the $^{13}C$ isotope of $D_1$.

*3.1.3 DabaAAA*

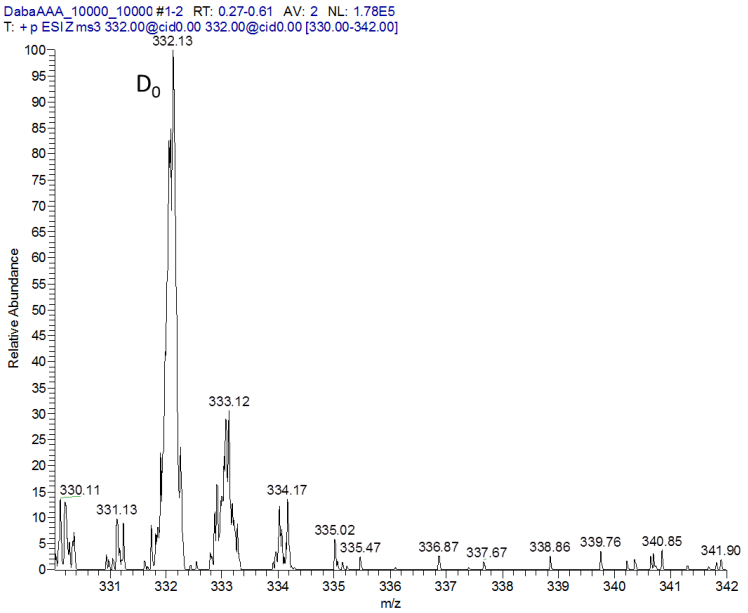


The HDX spectrum for DabaAAA shows that DabaAAA (M+H = 332) is present. There is no exchange seen in this data. The kinetic plot supports that the ion abundances have not changed over time. There is a relatively small peak at m/z= 333, which is from the $^{13}C$ isotope of DabaAAA.

*3.1.4 DapaAAA*

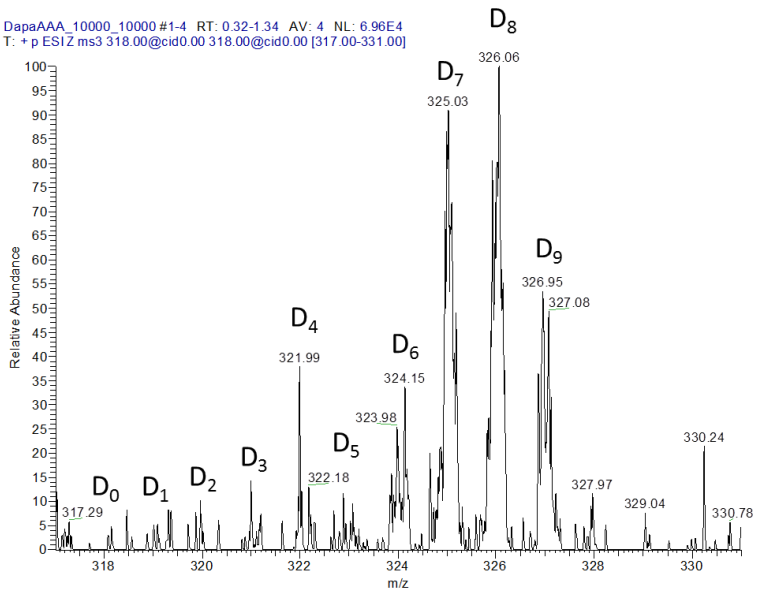


The HDX spectrum for DapaAAA shows that $D_0$ (M+H = 318) is no longer observed in the spectrum. Rather in this case, the molecule is exchanging up to nine deuterium atoms. There are nine possible exchangeable sites in DapaAAA and all exchanges were seen in this spectrum. As reported in a number of studies, the relative basicity of different sites follows: side chain amino N > N-terminal amino N > amide carbonyl O> carboxylic carbonyl O > amide [41]. For Dapa, the side chain and the N-terminus have very similar PAs [15, 17, 36, 41]. This suggests that the most labile hydrogens that exchange first are the hydrogens located on the N-terminus of DapaAAA, followed by the hydrogens on the side-chain residue due to the relay mechanism. DapaAAA has the lowest proton affinity and shortest chain length of the XAAA peptides and the data suggests that the side chain is close enough to exchange with the hydrogens on the amide back bones as well as the N-terminus [15, 17, 36].

## 3.2 Alanine-X-Alanine-Alanine

### *3.2.1 AKAA*

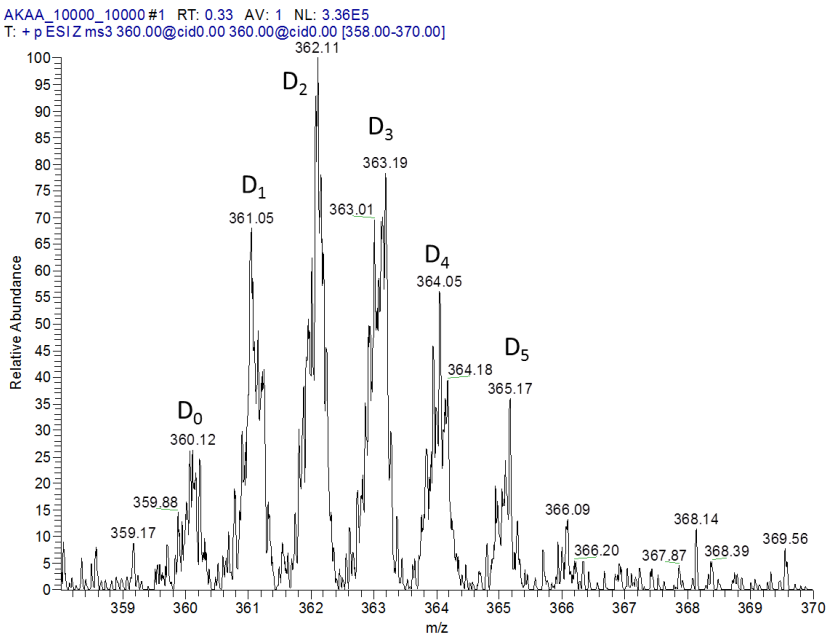


AKAA (M+H = 360) exchange up to $D_5$ ((M+H = 360) under our experimental conditions. This suggests that the five labile hydrogens are located at the N-terminus and the side chain, and HDX occurs through the relay mechanism.

*3.2.2 AOAA*

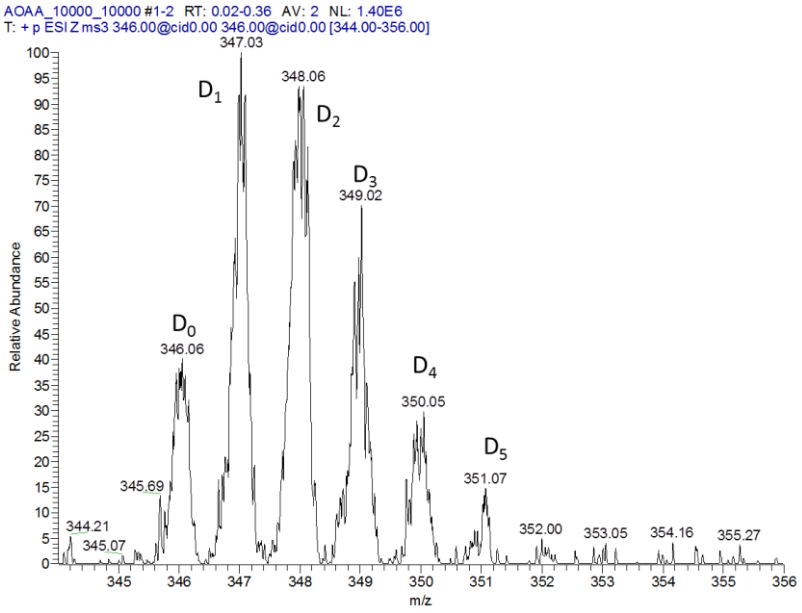

AOAA (M+H = 346) also exchanges up to $D_5$ (M+H = 351), similar to AKAA, suggesting that the five labile hydrogens are located at the N-terminus, and the side chain. Exchange again occurs through the relay mechanism.

### *3.2.3 ADabaAA*

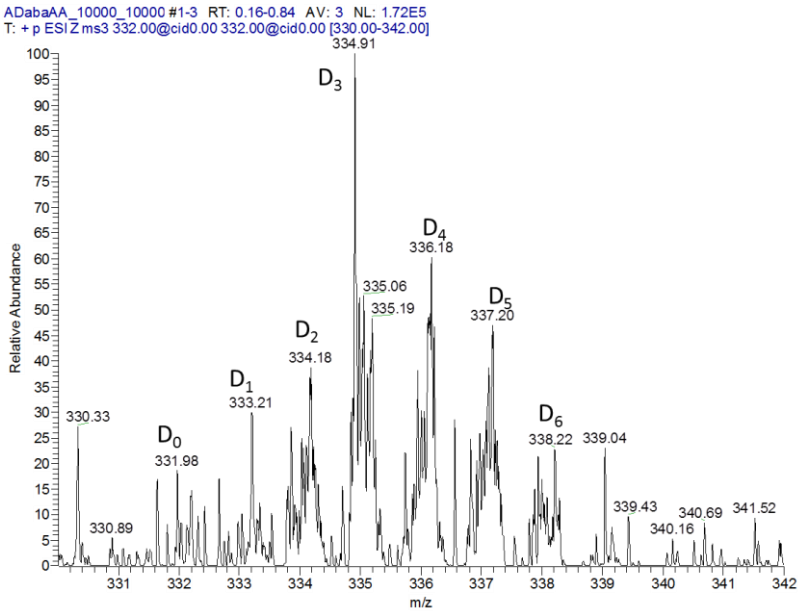


ADabaAA (M+H = 332) exchanges up to $D_6$ (M+H = 338). The number of exchanges suggests that the six labile hydrogens are located at the N-terminus, the side chain which occurs through the relay mechanism, and one exchange at the C-terminus though the flip flop mechanism.

### *3.2.4 ADapaAA*

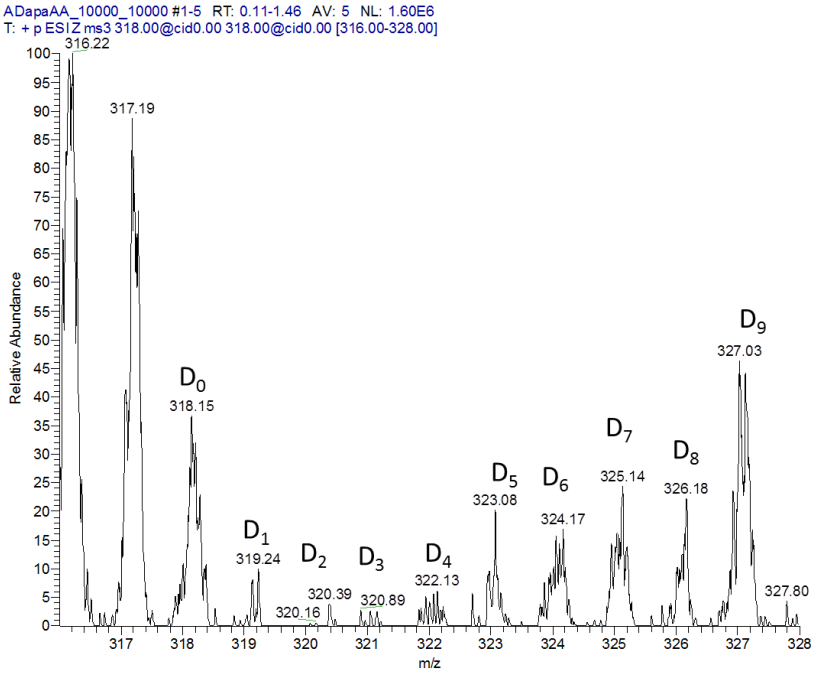


ADapaAA (M+H = 318) is present and exchange can be seen up to $D_9$ (M+H = 327). Number of exchanges suggests that the five labile hydrogens are located at the N-terminus, the side residue which occurs through the relay mechanism.

## 3.3 Alanine-Alanine-X-Alanine

### *3.3.1 AAKA*

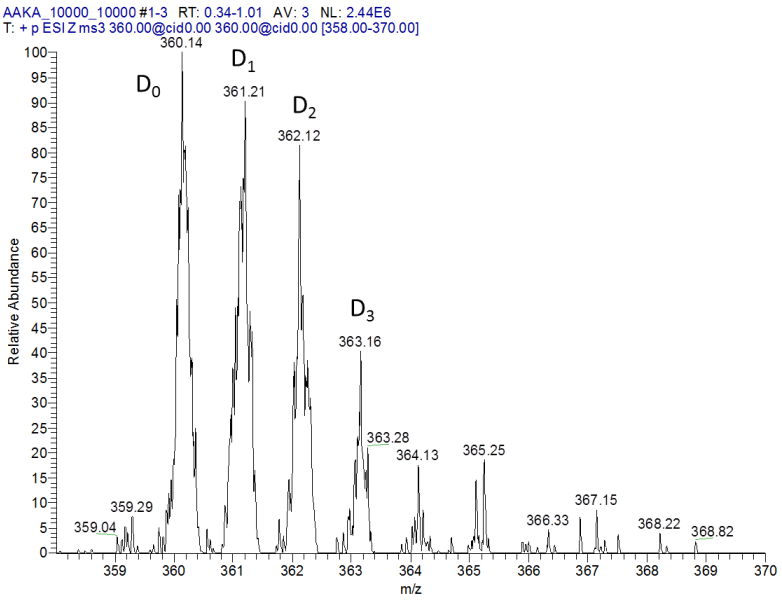


AAKA (M+H = 360) exchanges up to $D_3$ (M+H = 364). This exchange suggests that exchange occurs through the relay mechanism. Labile hydrogens are located at the N-terminus and side chain.

### *3.3.2 AAOA*

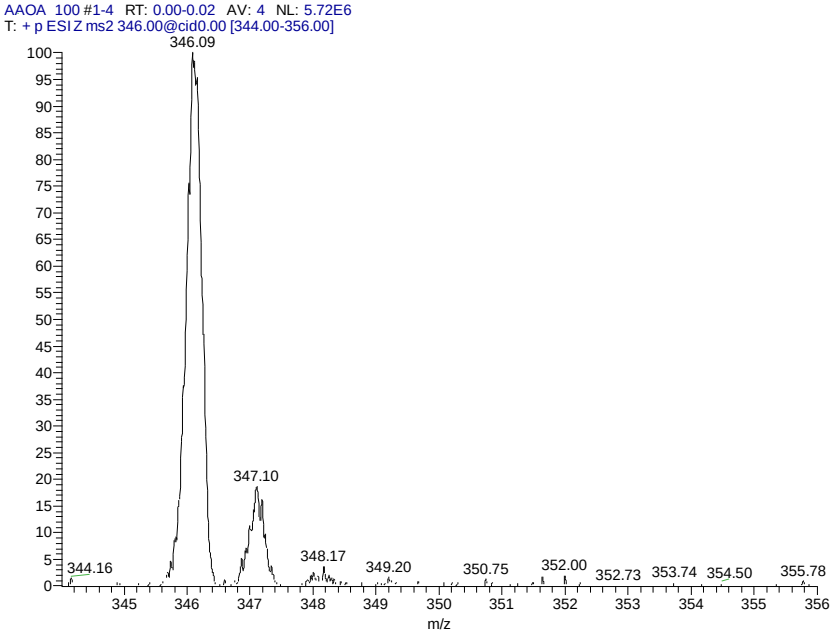

The HDX spectrum for AAOA shows that only $D_0$ (M+H = 346) is present. There is no exchange seen in this plot. The Kinetic plot Figure A.1 (in Appendix) similarly supports that the ion abundances have not changed drastically (relatively less than less 10% change) over (reaction) time. The peak at m/z= 347 is representative of presence of $^{13}C$.

### *3.3.3 AADabaA*

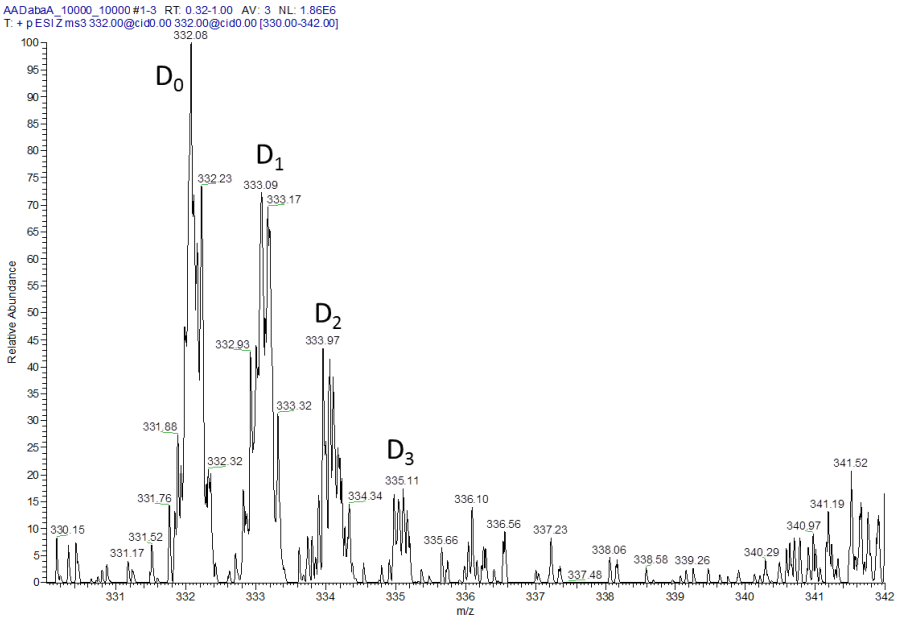


AADabaA (M+H = 332) exchanges can be seen up to $D_3$ (M+H = 335). This exchange suggests that exchange occurs through the relay mechanism. Labile hydrogens are located at the N-terminus and side chain.

### *3.3.4 AADapaA*

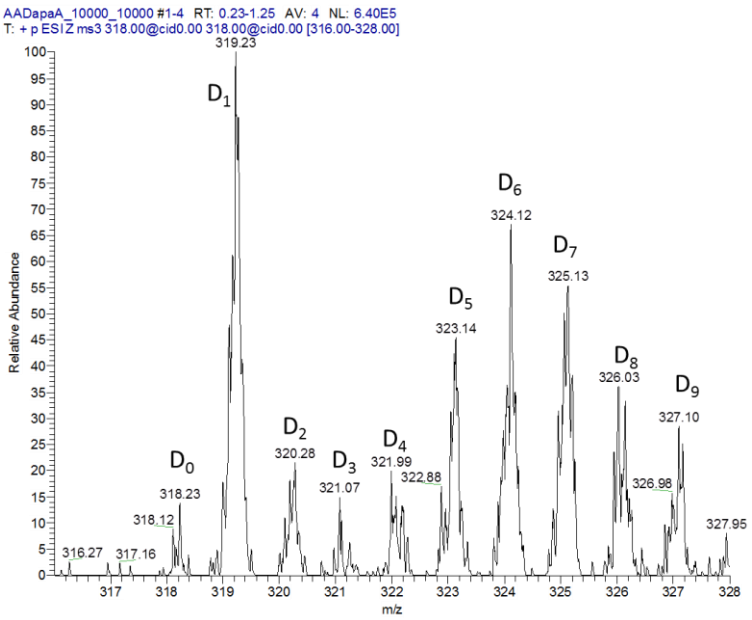


AADapaA (M+H = 318) exchanges up to $D_9$ (M+H = 327). This suggest that there are nine labile hydrogens are located at the N-terminus and the side chain which exchange occurs through the relay mechanism, and the C-terminus at which exchange is occurring though the flip flop mechanism. In addition, the high peak at $D_1$ (M+H= 319) suggests that there is a second population of ions that are exchanging once through the flip flop mechanism, and not undergoing the relay mechanism.

## 3.4 Alanine-Alanine-Alanine-X

### *3.4.1 AAAK*

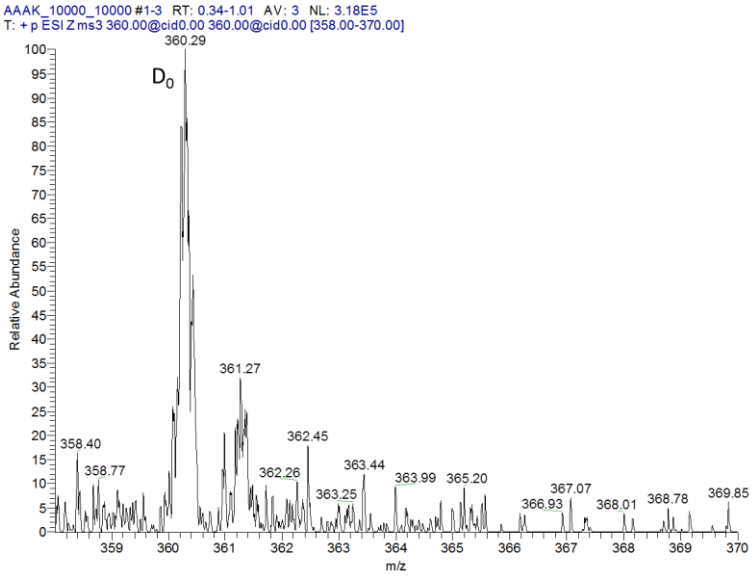


The HDX spectrum for AAAK shows that $D_0$ (M+H = 360) is present. There is no exchange seen in this plot. The kinetic plot (in Appendix) similarly supports that the ion abundances have not changes over (reaction) time. Peak at m/z= 361 is representative of present of $^{13}C$ .

*3.4.2 AAAO*

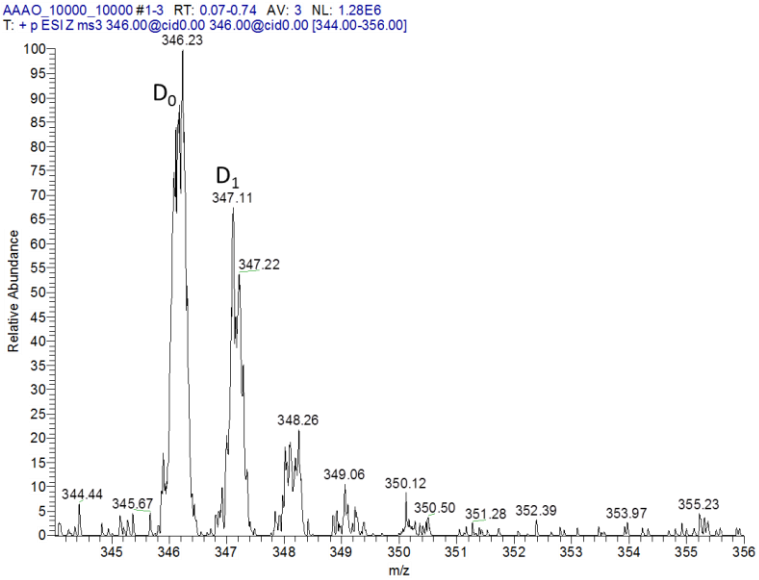

The HDX spectrum for OAAA (M+H = 346) shows one exchange seen in this plot at m/z=347. The kinetic plot (in the Appendix) similarly supports that there is one extremely slow exchange. This one labile hydrogen may be located on the C-terminus and exchange occurs through the flip-flop mechanism. There is a relatively small peak at m/z= 348, which is present of $^{13}C$.

### *3.4.3 AAADaba*

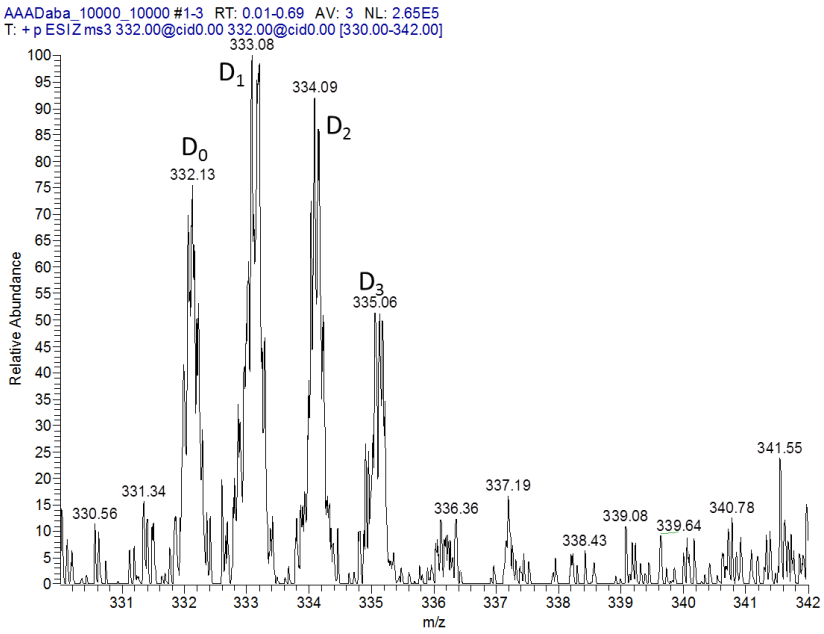


AAADaba (M+H = 332) exchanges up to $D_3$ (M+H = 335). This exchange suggests labile hydrogens are located at the N-terminus and side chain and exchange occurs through the relay mechanism.

### *3.4.4 AAADapa*

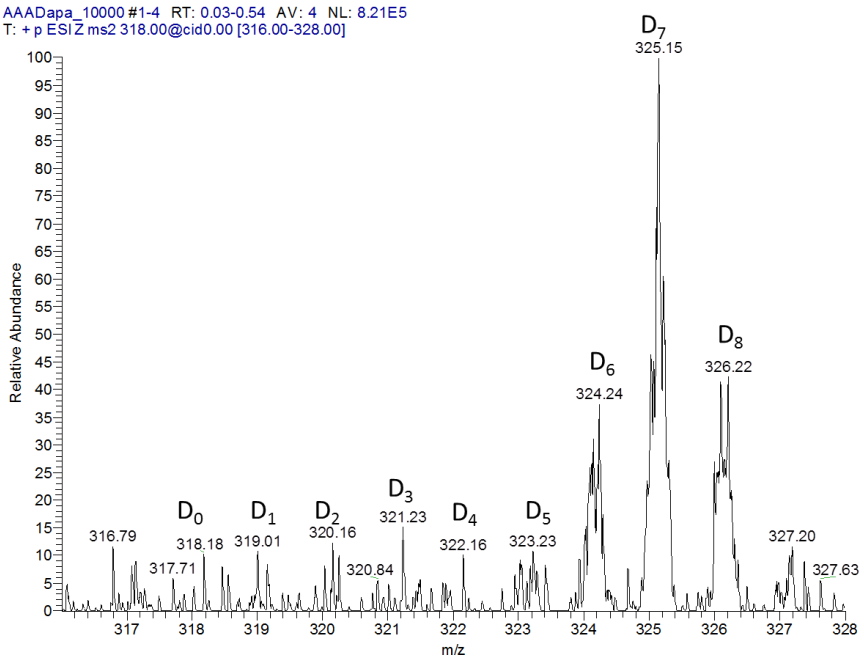


The HDX spectrum for AAADapa (M+H = 318) shows up to eight possible exchanges. This suggests that the most labile hydrogens that exchange first are the hydrogens located on the N-terminus of DapaAAA, followed by the hydrogens on the lysine residue due to the relay mechanism [22, 25], and followed by a flip flop mechanism at the carboxyl group.

### 3.5 X-Alanine$^+$ ($b_2^+$) ions

*3.5.1 KA$^+$*

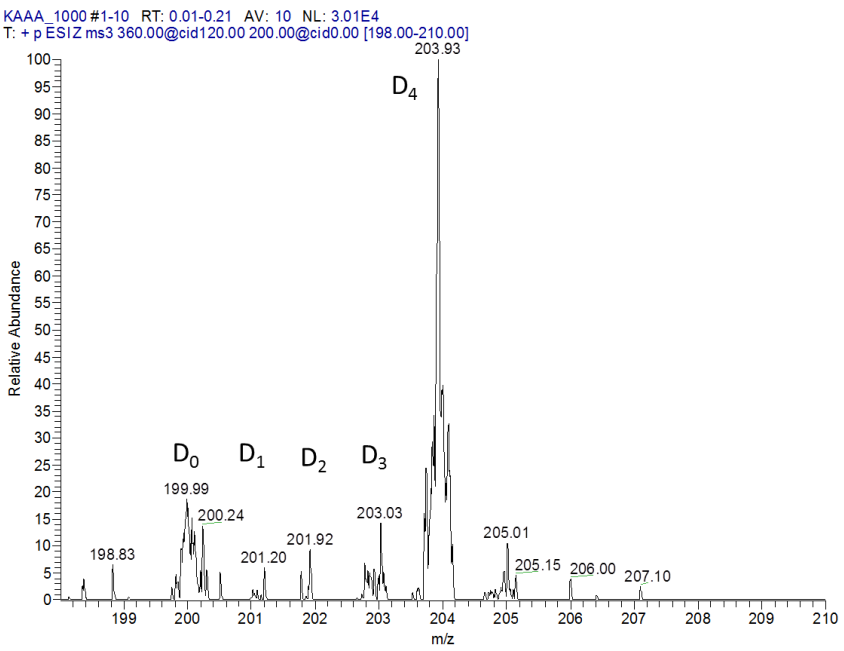


KA $b_2^+$ (M+H = 200) exchanges up to $D_4$ (M+H = 204). This ion had previously be shown to give four exchanges resulting from a diketopiperazine structure [15].This exchange suggests labile hydrogens are located at the side chain and nearest hydrogen on the amide backbone and exchange occurs through the relay mechanism. Spectra was obtained from a $D_2O$ flow rate of 200µL/hr.

### *3.5.2 DabaA*$^+$

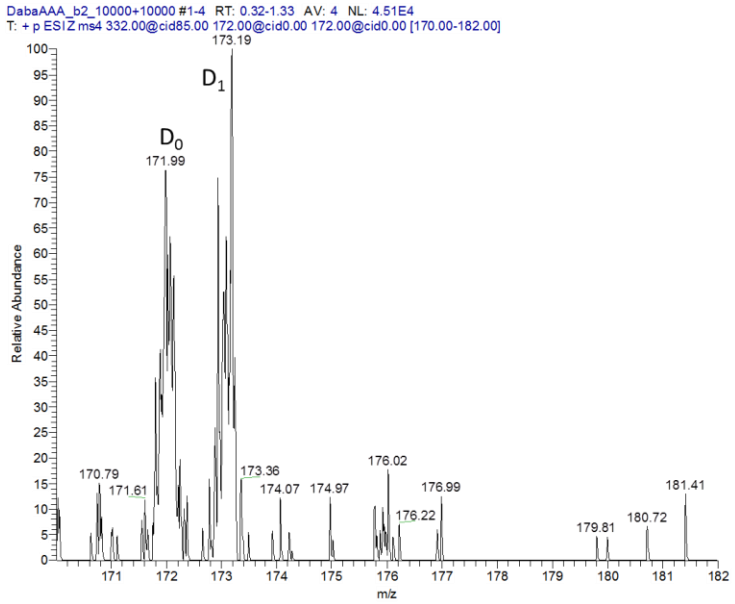


This spectra was obtained from a $D_2O$ flow rate of 400µL/hr. $DabaA^+$ (M+H =172) exchanged once. This structure was confirmed by Wysocki et al, that $DabaA^+$ due to its shorter chain length, is unable to facilitate HDX as well as lysine. It was also confirmed as a diketopepirazine structure through IRMPD [15].

### *3.5.3 $DapaA^+$*

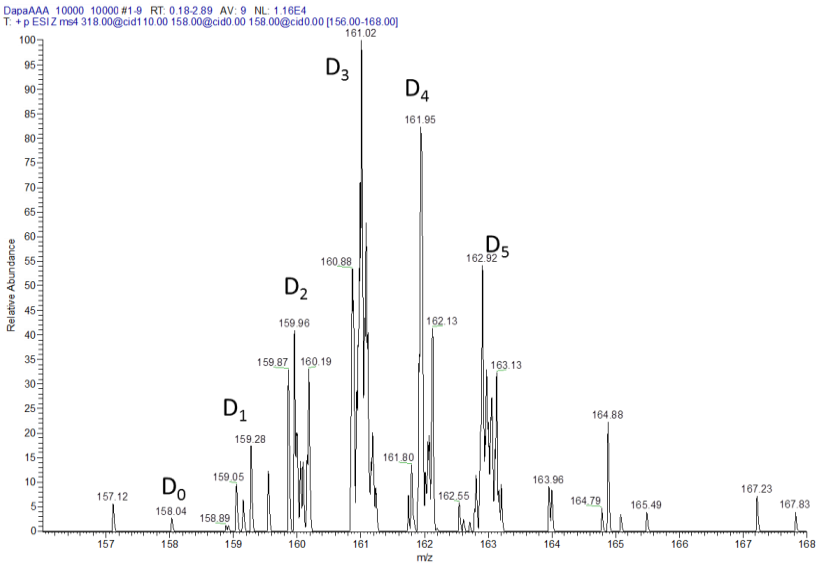


$DapaA^+$ (M+H= 158) exchanges up to $D_5$ (M+H= 163) suggesting five labile hydrogens.

## 3.6 Alanine-X$^+$ ($b_2^+$) ions

### *3.6.1 AK$^+$*

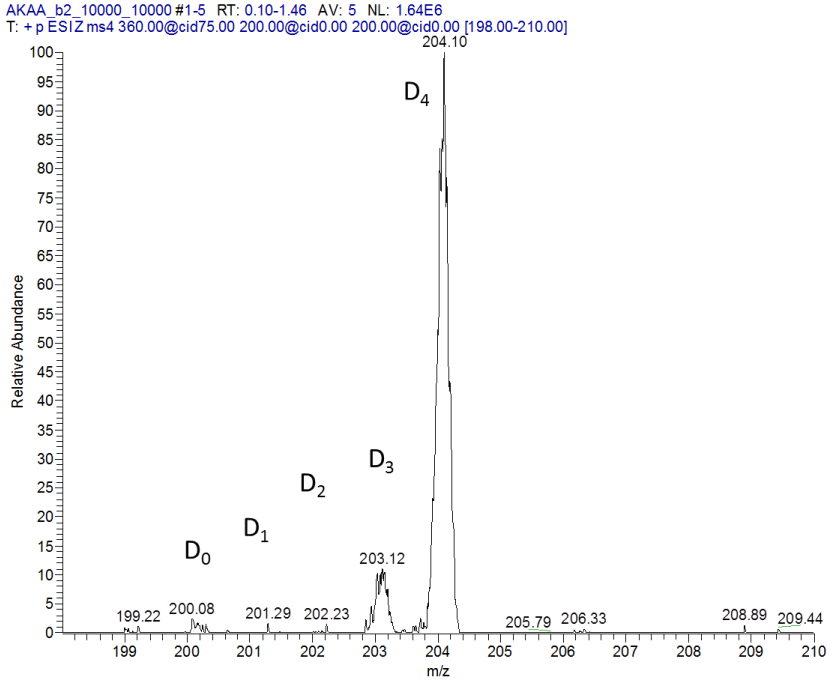


AK$^+$ (M+H = 200) exchanges up to $D_4$ (M+H = 204) suggesting four labile hydrogens.

### *3.6.2 AO$^+$*

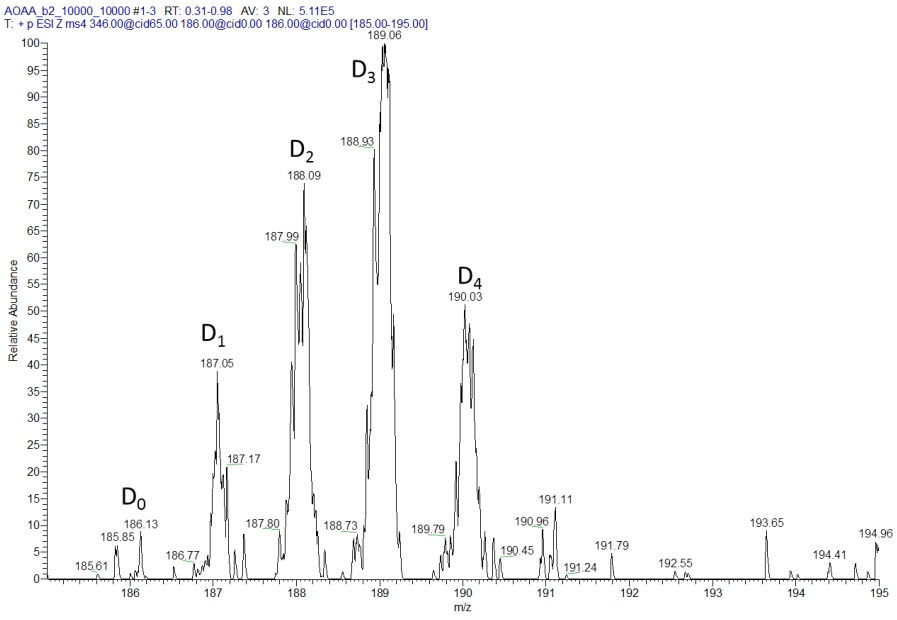

$AO^+$ (M+H = 187) exchanges up to $D_4$ (M+H = 190) suggesting four labile hydrogens.

### *3.6.3 ADaba*$^+$

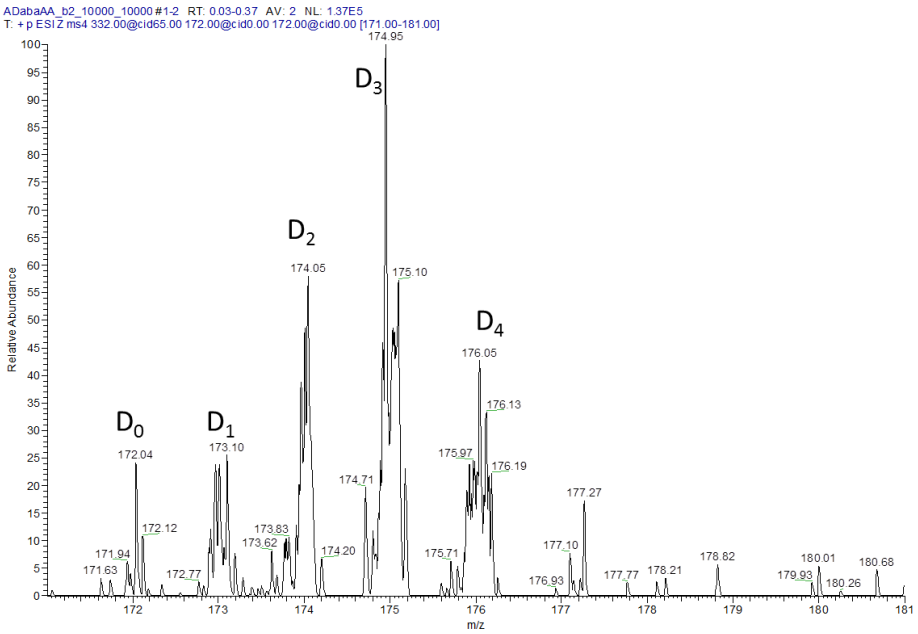


ADaba$^+$ (M+H = 172) is present and and exchange can be seen up to $D_4$ (M+H = 176) suggesting four labile hydrogens.

## 3.7 Alanine-Alanine-X$^+$ ($b_3^+$) ions

### *3.7.1 AAK*$^+$

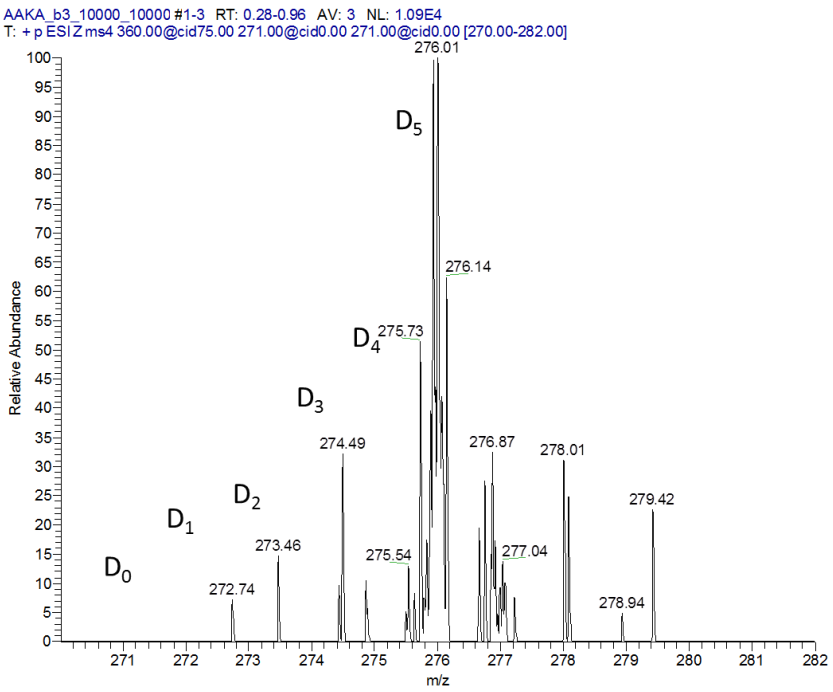


$AAKA^+$ (M+H = 271) exchanges up to $D_5$ (M+H = 276) suggesting five labile hydrogens. There is a relatively small peak at m/z= 277, which is present of $^{13}C$

*3.7.2 $AAO^+$*

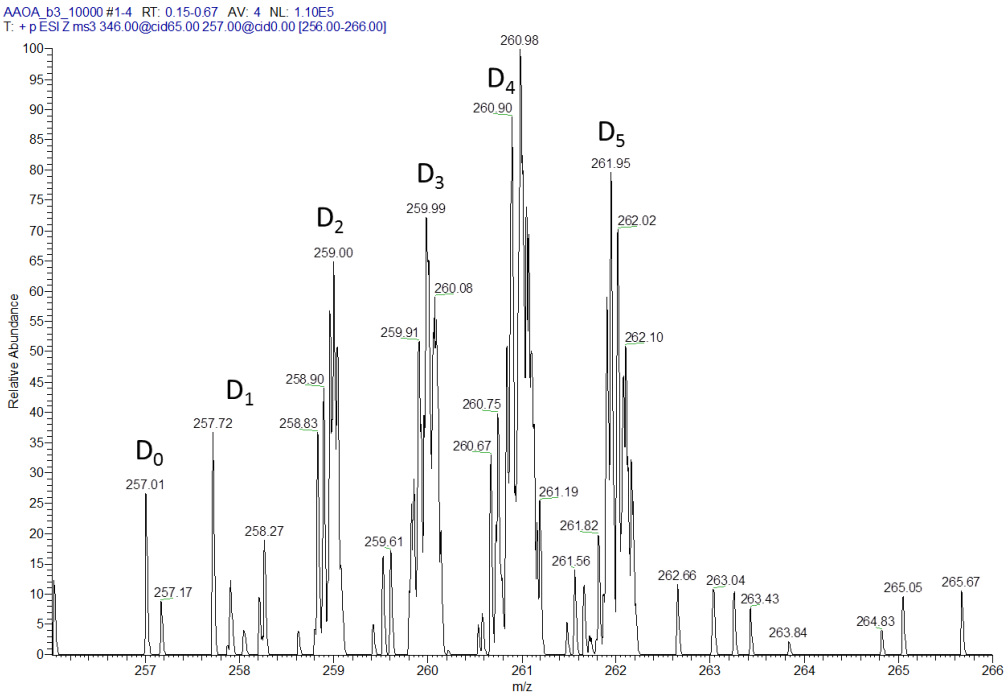


$AAO^+$ (M+H = 257) exchanges up to $D_5$ (M+H = 262) suggesting five labile hydrogens.

### *3.7.3 AADaba*$^+$

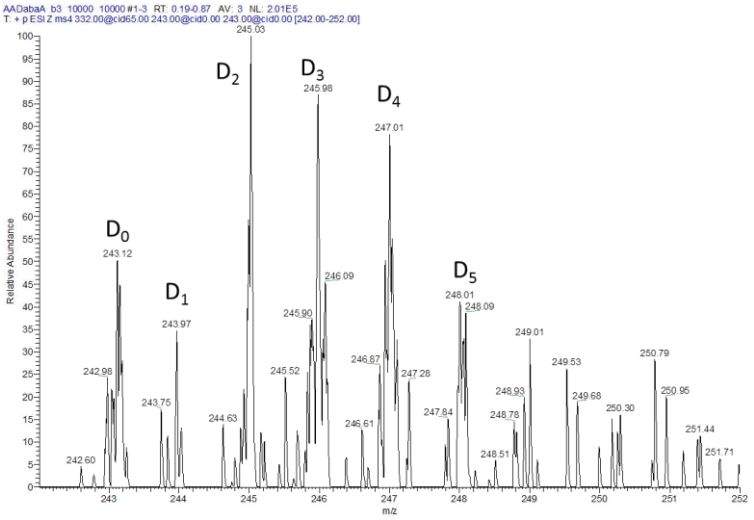


AADaba$^+$ (M+H = 243) exchanges up to $D_5$ (M+H = 247) suggesting five labile hydrogens.

### *3.7.4 AADapa*$^+$

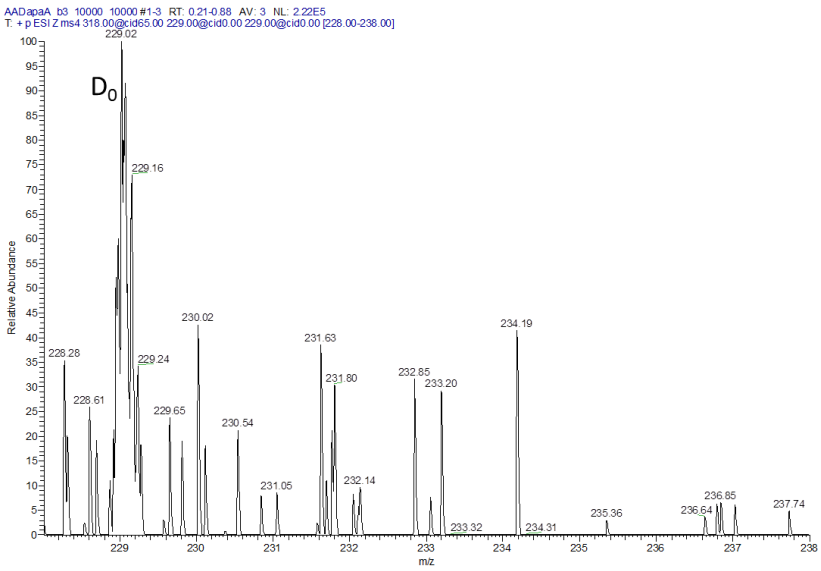


AADapa$^+$ (M+H = 229) does not exchange.

# Chapter 4: Discussion

## 4.1 Tetrapeptides

Below are tables assembled from summarizing total exchanges, for each tetrapeptide, as discussed in previously mentioned results:

**Table 1: Total Exchanges for Tetrapeptides of Lysine and its Homologs.**

| Tetrapeptide Position | XAAA | AXAA | AAXA | AAAX |
|---|---|---|---|---|
| Lysine | DNE | 5 | 3 | DNE |
| Ornithine | 1 | 5 | DNE | 1 |
| Daba | DNE | 6 | 3 | 3 |
| Dapa | 9 | 9 | 9 | 8 |

Studies have suggested that the hydrogen bond between the side chain and the N-terminus puts these two groups in an ideal position for undergoing exchange via the relay mechanism; however, the water must first insert into the hydrogen bond [24]. HDX can be suppressed if the relay site is sterically hindered or by formation of cyclic intermediates involving the deuterating reagent [24, 36]. If the hydrogen bond is too strong, it will be energetically unfavorable for a $D_2O$ molecule to enter the relay site [36]. Literature has shown that that proton affinity correlates with a number of other properties such as shortening the side-chain of the probe residu e, which causes the flexibility needed to form intramolecular hydrogen bonds to decrease. Batoon and Ren (2016) have suggested that the lysine side chain may curve towards the backbone carbonyl group and forms the O--- $NH_3^+$---O hydrogen bonding motif [22, 24, 36]. Another property correlated with proton affinity is the polarizability decrease due to the

removal of $-CH_2-$ group in the side chain, and the decrease in accessible surface area [22,24]. Furthermore, Poutsma and coworkers showed that the three protonated peptides, $LysH^+$ , $OrnH^+$, and $DabaH^+$ , adopted a cyclized hydrogen bridge motif, between its side chain and N-terminus, whereas $DapaH^+$ could not [24, 36]. This is fairly consistent with data presented in this study as seen in Table 1, Dapa-containing peptides exchange regardless of position suggesting that the short side chain can form weak hydrogen bonds with backbone CO groups, whereas lysine, ornithine, and Daba-containing tetrapeptides have stronger intramolecular hydrogen bonding schemes and a resistant to exchange. Nevertheless, the prevalence of exchanges suggest that Dapa has many labile hydrogens and can potentially form a variety of intermolecular hydrogen bonds.

Ornithine-containing peptides tend to resist exchange, exchanging only once via the flip flop mechanism or not at all, except when the residue is at the second position. These results suggest that ornithine may have a very strong or very weak hydrogen bonding scheme depending on position. No exchange and exchange via flip flop suggest that the N-terminus and the side chains can form strong intramolecular bonds at the first and last positions. Lysine located near the N- or C-terminus is also shows strong hydrogen bonding motifs. Lysine is the longest side chain and is more flexible and more able to adopt optimal geometry for hydrogen bonding [24]. Daba-containing tetrapeptide show no exchange when located at the N-terminus which suggest an optimal side chain length for internal hydrogen bonding when the X residue is at the N-terminus.

AXAA tetrapeptides shows the highest level of exchanges indicating a favorable distance for HDX for all side chains, and possibly a weak internal hydrogen bonding schemes when residues are located at the second position.

### 4.2 Tetrapeptide Fragments

**Table 2: Total Exchanges for Tetrapeptides Fragments**

| $b_n^+$ | $XA^+$ | $AX^+$ | $AAX^+$ |
|---|---|---|---|
| Lysine | 4 | 4 | 5 |
| Ornithine | N/A | 4 | 5 |
| Daba | 1 | 4 | 5 |
| Dapa | 5 | N/A | DNE |

A study conducted by Gucinski et al [15] confirmed with infrared multiphoton dissociation (IRMPD) spectroscopy that $KA^+$ and $DabaA^+$ are exclusively diketopiperazine structures [15]. They suggest that the availability of protonated side chain nitrogens facilitates the formation of the diketopiperazine structure by providing a protonated nitrogen in a location that can allow for charge stability and bridging to the nitrogen (or carbonyl oxygen for Daba) of the XxxAla amide bond, which facilitates the *trans-cis* isomerization necessary for diketopiperazine formation [15]. Using an FTICR mass spectrometer, they showed that $DabaA^+$ exchanged once and $KA^+$ exchanged four times. The four total deuterium atoms are observed to incorporate into the KA $b_2^+$ ion structure, three hydrogens are from the side chain, whereas the fourth deuterium incorporated at a backbone amide nitrogen location. $DabaA^+$ exhangne is different because of its short chain, bridging occurs bwtween the side residue the carbonyl oxygen [15].

In a study conducted by Perkins et al., the authors conducted IRMPD spectroscopy studies on $HA^+$ and results show that it is possible that oxazolone and diketopiperazine strucutres

can both be formed. In the diketopiperazine structure, the $D_2O$ bridges from the nitrogen in the histidine side chain to the neighboring carbonyl oxygen, consistent with exchange of one hydrogen similar to the exchange meachsim in $DabaA^+$ and seen in figure 4.1. Whereas the oxazolone strucutre can exchange three hydrogens due to the $D_2O$ bridging between the backbone nitrogen, and the nitrogen in the histidine side chain, which allows for up to three exchanging hydrogen [17].

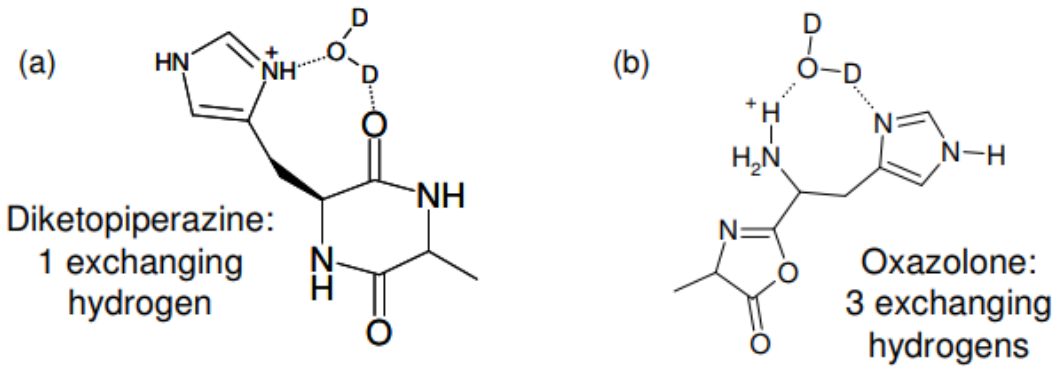


**Figure 4.1: Relay mechanism for a) diketopiperazine and b) oxazolone. Adapted from [41]**

In this study, AX $b_2^+$ ions all exchange 4 hydrogens consistent with the diketopiperazine structure. It may be possible for $DapaA^+$ to exhibit similar behavior. AAX $b_3^+$ ions also show similar HDX behavior. However, results need to be compared to results obtained from infrared multiphoton dissociation (IRMPD) to confirm the structures of b ions [17].

Studies have shown that ornithine can form lactams from a nucleophilic attack of the carbonyl carbon by the amine side chain to form a six-membered lactam. The mechanism for this 'ornithine effect' can be applicable to lysine residues. However, the formation of a seven-membered lactam ring is less favored, and the effect may be weaker in lysine residues [21].

Although the mechanism of exchange is unclear for lactams, many studies support that the relay mechanism is the method of exchange for cyclic structures [7, 41-43].

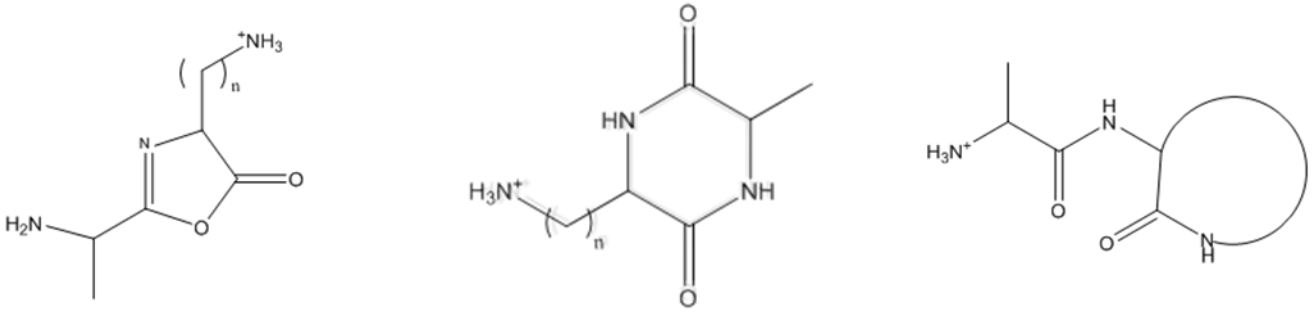


**Figure 4.2: Possible for structures $AX^+$ b ions: oxazolone (right); diketopiperazine (middle); lactam (right)**

Possible b ion structures are seen above in Figure 4.2, the relay mechanism will remain the main mechanism of hydrogen deuterium exchange. For an oxazolone structure, there are 5 labile hydrogens but there may be up to three possible exchanges through relay mechanism if the side change interacts with the carbonyl in the ring [17]. For the diketopiperazine structure, there are five labile hydrogens, but depending on the length of the side chain, only four (or one exchange similar to $HA^+$ and $DabaA^+$) may be accessible [17]. Lactams have 5 labile hydrogens, as seen in figure 4.2.

HDX results served as an indirect method to probe structure. Results suggest that b ion structures are either diketopiperazine or lactam. Further work such as using IRMPD spectroscopy is necessary to provide evidence of b ion structure.

### 4.3 Future Work

Current work involves completing density functional theory calculations on the structures of the tetrapeptides and their $b_2^+$ and $b_3^+$ ions. The HDX results will be combined with IRMPD experiments to provide information on the structure and H-bonding abilities of these peptides. In

addition, we are looking at tetrapeptides containing arginine or its oxy-analog canavanine in varying positions. Other current work is performing HDX with synthesized diketopiperazine structures and lactams with lysine and its homologs to compare our HDX results.

Future works includes looking at HDX of histidine and arginine containing peptides to compare the differences in behaviors of these basic side chains. Studying the fragmentation patterns of larger lysine and lysine analog containing peptides will provide more insight into the mechanisms of ion formation at play. Analyzing the fragmentation mechanisms of peptides that are 9 or 10 amino acids long which contain lysine or arginine at the C-terminus are particularly relevant to tryptic digests and bottom-up proteomics research. Finally, it will be beneficial to look at doubly protonated lysine species, and expand research to arginine containing peptides to discern fragmentation mechanisms and ensure a robust proteomics experiment.

References

[1] Abu-Jamous B; Fa R; Nandi AK. Central Dogma of Molecular Biology. In *Integrative Cluster Analysis in Bioinformatics*; John Wiley & Sons, Ltd.; 2015; pp. 33-52.

[2] Pandey, Akhilesh, and Matthias Mann. "Proteomics to study genes and genomes." *Nature* **2000**, 405, 837-846.

[3] Aebersold R; Mann M. Mass spectrometry-based proteomics. *Nature*. **2003**, 422, 198-207.

[4] Weston, A. D.; Hood, L. Systems biology, proteomics, and the future of health care: toward predictive, preventative, and personalized medicine. *Journal of Proteome Research*. **2004**, 3, 179-196.

[5] Hasan, Z.I. Fragmentation Studies of Lysine and Lysine Analog Containing Tetrapeptides. B.S. Honors, College of William and Mary, Williamsburg, VA, 2016.

[6] Catherman AD, Skinner OS, Kelleher NL. Top down proteomics: facts and perspectives. *Biochemical and biophysical research communications*. **2014**, 445, 683-93.

[7] Paizs, B.; Suhai, S. Fragmentation pathways of protonated peptides. *Mass Spectrometry Reviews*. **2005**, 24, 508-548

[8] Dongre, A. R.; Jones, J. L.; Somogyi, Á.; Wysocki, V. H. Influence of peptide composition, gas-phase basicity, and chemical modification on fragmentation efficiency: Evidence for the mobile proton model. *Journal of the American Chemical Society*. **1996**, 118, 8365-8374.

[9] Ho C.S.; Lam C.W.; Chan M.H.; Cheung R.C.; Law L.K.; Lit L.C.; Ng K.F.; Suen M.W. Tai H.L. Electrospray ionisation mass spectrometry: principles and clinical applications. *The Clinical Biochemist Reviews*. **2003**, 24, 3.

[10] Fenn J.B.; Mann M; Meng C.K.; Wong S.F.; Whitehouse C.M. Electrospray ionization for mass spectrometry of large biomolecules. *Science*. **1989**, 246, 64-71.

[11] Vaisar T; Urban J. Low-energy collision induced dissociation of protonated peptides. Importance of an oxazolone formation for a peptide bond cleavage. *European Mass Spectrometry*. **1998**, 5, 359-64.

[12] Wysocki V.H.; Tsaprailis G; Smith L.L.; Breci L.A.. Mobile and localized protons: a framework for understanding peptide dissociation. Journal of Mass Spectrometry. **2000**, 35, 1399-406.

[13] Polfer N.C.; Oomens J; Suhai S; Paizs B. Spectroscopic and theoretical evidence for oxazolone ring formation in collision-induced dissociation of peptides. *Journal of the American Chemical Society*. **2005**; 127, 17154-5.

[14] Morrison L.J.; Chamot-Rooke J; Wysocki V.H. IR action spectroscopy shows competitive oxazolone and diketopiperazine formation in peptides depends on peptide length and identity of terminal residue in the departing fragment. *Analyst*. **2014**, 139, 2137-43.

[15] Gucinski A.C,; Chamot-Rooke J; Nicol E, Somogyi Á; Wysocki V.H. Structural influences on preferential oxazolone versus diketopiperazine b2+ ion formation for histidine analogue-containing peptides. *The Journal of Physical Chemistry A*. **2012**, 116, 4296-304.

[16] Pal D; Chakrabarti P. Cis peptide bonds in proteins: residues involved, their conformations, interactions and locations. *Journal of molecular biology*. **1999**, 294, 271-88.

[17] Perkins B.R.; Chamot-Rooke J; Yoon SH; Gucinski A.C.; Somogyi A; Wysocki V.H. Evidence of diketopiperazine and oxazolone structures for HA b2+ ion. *Journal of the American Chemical Society*. **2009**; 131,17528-9.

[18] Farrugia J.M.; Richard A.J.; Reid G.E. Do all b2 ions have oxazolone structures? Multistage mass spectrometry and ab initio studies on protonated N-acyl amino acid methyl ester model systems. *International Journal of Mass Spectrometry*. **2001**, 210, 71-87.

[19] Raulfs; M. D. M.; Breci, L., Bernier; M., Hamdy; O. M., Janiga, A.; Wysocki, V.; Poutsma, J. C. Investigations of the mechanism of the "proline effect" in tandem mass spectrometry experiments: The "pipecolic acid effect". *J. Am. Soc. Mass Spectrom*.; 2014, 25,

[20]Huang, Y.; Wysocki, V.; Tabb, D.; Yates, J. I. The influence of histidine on cleavage C-teriminal to acidic residues in doubly protonated tryptic peptides. *Int. J. Mass Spectrom*. **2002**. 219, 233-244.

[21] McGee W.M.; McLuckey S.A. The ornithine effect in peptide cation dissociation. *Journal of Mass Spectrometry*. **2013**, 48, 856-61.

[22] Schroeder O.E.; Andriole E.J.; Carver K.L.; Colyer K.E.; Poutsma J.C. Proton affinity of lysine homologues from the extended kinetic method. *The Journal of Physical Chemistry A*. **2004**, 108, 326-32.

[23] Moser A; Range K; York D.M. Accurate proton affinity and gas-phase basicity values for molecules important in biocatalysis. *The Journal of Physical Chemistry B*. **2010**, 114, 13911-21.

[24] Batoon P; Ren J. Proton Affinity of Isomeric Dipeptides Containing Lysine and Non-Proteinogenic Lysine Homologues. *The Journal of Physical Chemistry B*. **2016**. 120, 7783-94.

[25] Campbell S; Rodgers M.T.; Marzluff E.M.; Beauchamp J.L. "Deuterium-Exchange Reactions as a Probe of Biomolecule Structure-Fundamental-Studies of CAS Phase H/D Exchange-Reactions of Protonated Glycine Oligomers with $D_2O$, $CD_3OD$, $CD_3CO_2D$, and $ND_3$." Journal of the American Chemical Society; **1995**, 117, 12840-12854

[26] Rozman, M. "The gas-phase H/D exchange mechanism of protonated amino acids." *Journal of the American Society for Mass Spectrometry*; **2005**, 16, 1846-1852.

[27] Stawikowski, M.; Fields, G.B. Introduction to peptide synthesis. *Current Protocols in Protein Science*, 2002, unit 18.1.

[28] Santini R.; Griffith M.C.; Qi M. A measure of solvent effects on swelling of resins for solid phase organic synthesis. *Tetrahedron letters*. **1998**, 39, 8951-4.

[29] Love, B.W. Love SYNTHESIS AND CHARACTERIZATION OF TIME-RESOLVED LANTHANIDE (III) LUMINESCENT PROBES FOR POTENTIAL DETECTION OF MELANOMA SKIN CANCER. Masters, Western Carolina University, Cullowhee, NC, 2017.

[30] Yu H.M.; Chen S.T.; Wang K.T. Enhanced coupling efficiency in solid-phase peptide synthesis by microwave irradiation. *The Journal of Organic Chemistry*. **1992**, 57, 4781-4.

[31] Pedersen SL, Tofteng AP, Malik L, Jensen KJ. Microwave heating in solid-phase peptide synthesis. *Chemical Society Reviews*. **2012**; 41, 1826-44.

[32] Valeur E, Bradley M. Amide bond formation: beyond the myth of coupling reagents. *Chemical Society Reviews*. **2009**; 38, 606-31.

[33] Straus, R.N. Fragmentation Studies of Lysine and Lysine Analog Containing Tetrapeptides. B.S. Honors, College of William and Mary, Williamsburg, VA, 2012.

[34] Ichou F; Schwarzenberg A; Lesage D; Alves S; Junot C; Machuron-Mandard X; Tabet J.C. Comparison of the activation time effects and the internal energy distributions for the CID, PQD and HCD excitation modes. Journal of Mass Spectrometry. **2014**; 49, 498-508.

[35] Nicoll, J. B.; Dearden, D. V. *KinFit*, 1.0 ed. (a computer program) Department of Chemistry and Biochemistry, Brigham Young University, Provo, UT, 1997).

[36] Arrington J.V.; Straus R.N.; Reynolds P.F.; Poutsma J.L.; Marzluff E.M.; Poutsma J.C. Gas-phase hydrogen deuterium exchange behavior of lysine and its homologs. *International Journal of Mass Spectrometry*. **2012,** 330, 200-6.

[37] Rožman M. Aspartic acid side chain effect—Experimental and theoretical insight. *Journal of the American Society for Mass Spectrometry*. **2007**, 18, 121-7.

[38] Green M.K.; Lebrilla C.B. The role of proton-bridged intermediates in promoting hydrogen-deuterium exchange in gas-phase protonated diamines, peptides and proteins. International Journal of Mass Spectrometry and Ion Processes**. 1998**,175, 15-26.

[39] Carr S.R.; Cassady C.J. Gas-phase basicities of histidine and lysine and their selected di-and tripeptides. *Journal of the American Society for Mass Spectrometry*. **1996**, 7, 1203-10.

[40] Xue G; Liu Z; Wang L, Zu L. The role of basic residues in the fragmentation process of the lysine rich cell-penetrating peptide TP10. *Journal of Mass Spectrometry*. **2015**, 50, 220-7.

[41] Chen X; Yu L; Steill J.D.; Oomens J; Polfer N.C. Effect of peptide fragment size on the propensity of cyclization in collision-induced dissociation: oligoglycine b2− b8. *Journal of the American Chemical Society*. **2009**, 131, 18272-82.

[42] Chen X; Tirado M; Steill J.D.; Oomens J; Polfer N.C. Cyclic peptide as reference system for b ion structural analysis in the gas phase. *Journal of Mass Spectrometry*. **2011**, 46, 1011-5.

[43] Kang Y; Terrier P; Ding C; Douglas D.J. Solution and gas-phase H/D exchange of protein–small-molecule complexes: cex and its inhibitors. *Journal of the American Society for Mass Spectrometry*. **2012**, 23, 57-67.

[44] Joyce J.R.; Richards D.S. Kinetic control of protonation in electrospray ionization. *Journal of the American Society for Mass Spectrometry*. **2011**, 22, 360-8.

[45] Paizs B, Suhai S. Towards understanding the tandem mass spectra of protonated oligopeptides. 1: mechanism of amide bond cleavage. *Journal of the American Society for Mass Spectrometry*. **2004**, 15,103-13.

[46] March R.E.; Todd J.F. *Practical aspects of trapped ion mass spectrometry, volume IV: Theory and instrumentation*. CRC press; 2010 May 25.

# Appendix

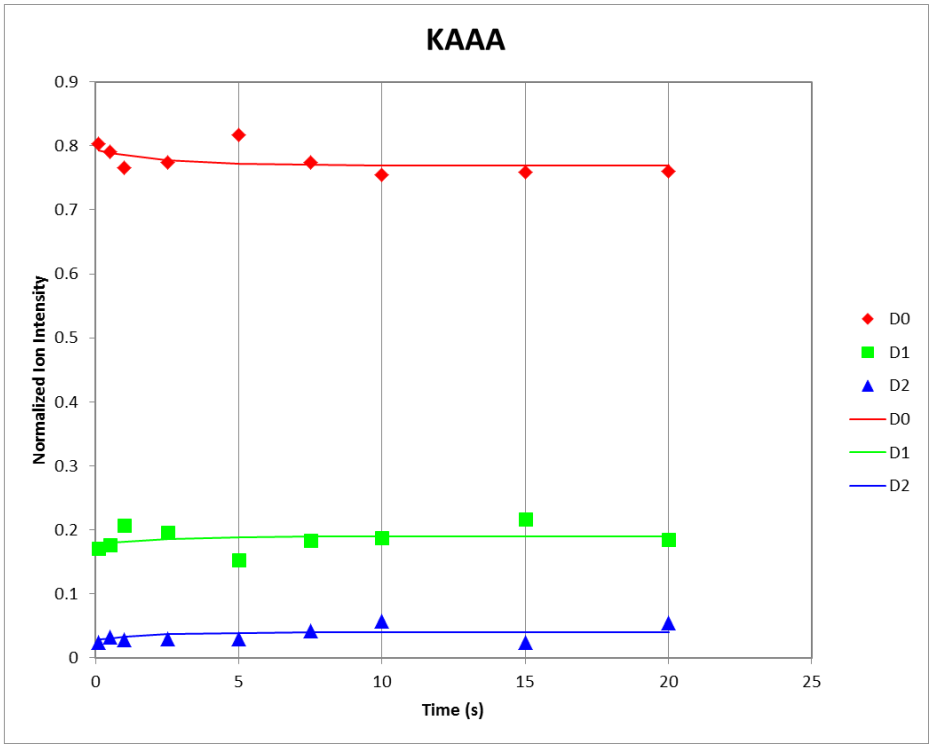
KAAA
Normalized Ion Intensity
Time (s)
0
0.1
0.2
0.3
0.4
0.5
0.6
0.7
0.8
0.9
0
5
10
15
20
25
D0
D1
D2
D0
D1
D2

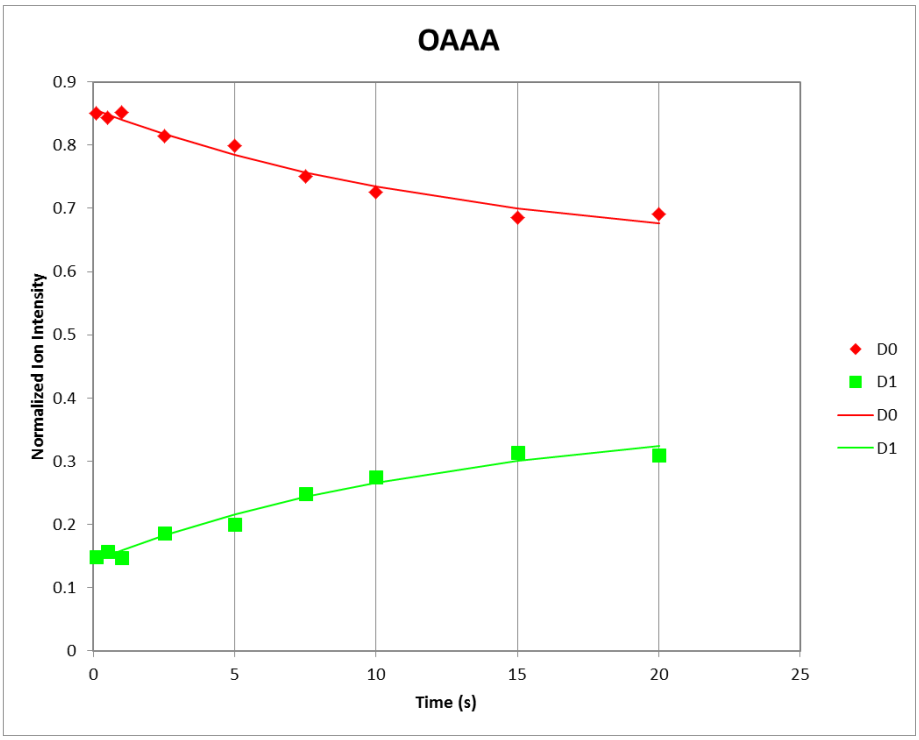
OAAA
Normalized Ion Intensity
Time (s)
0
0.1
0.2
0.3
0.4
0.5
0.6
0.7
0.8
0.9
0
5
10
15
20
25
D0
D1
D0
D1

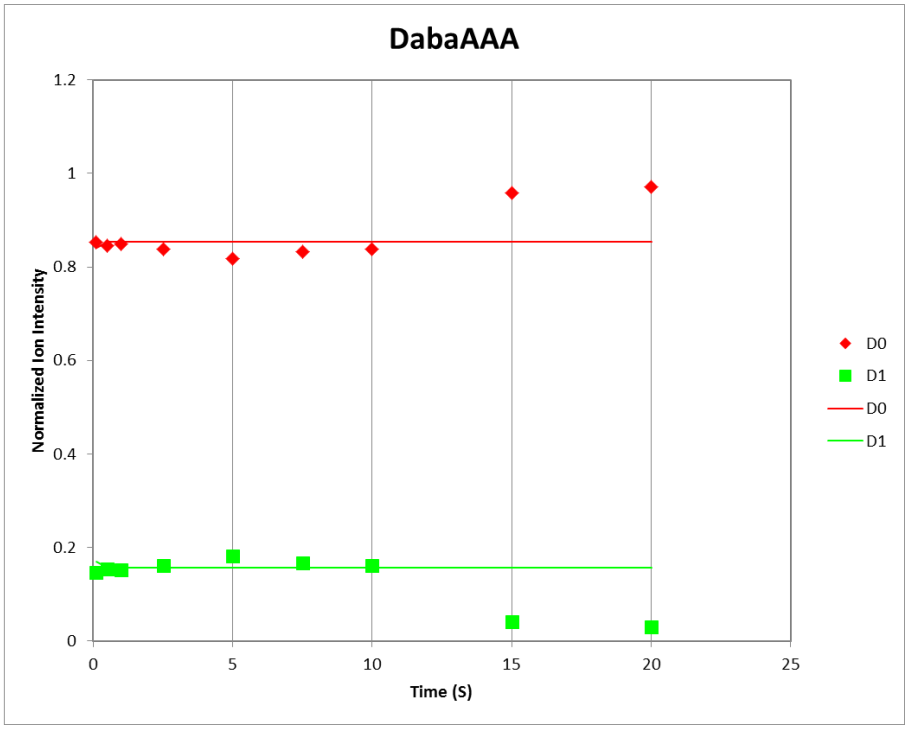
DabaAAA
Normalized Ion Intensity
Time (S)
D0
D1
D0
D1

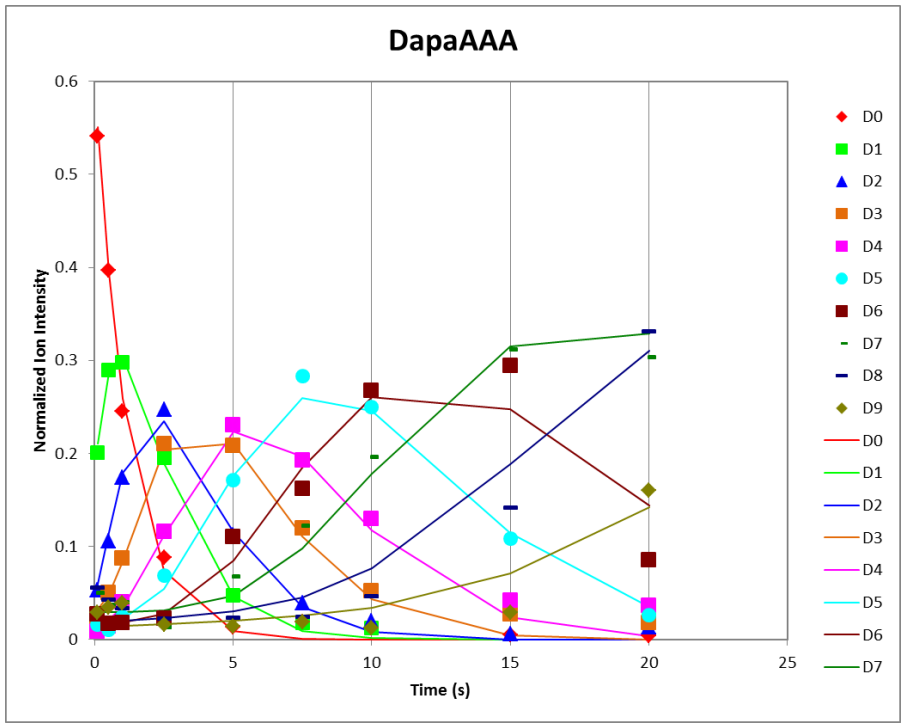
DapaAAA
Normalized Ion Intensity
Time (s)
D0
D1
D2
D3
D4
D5
D6
D7
D8
D9
D0
D1
D2
D3
D4
D5
D6
D7

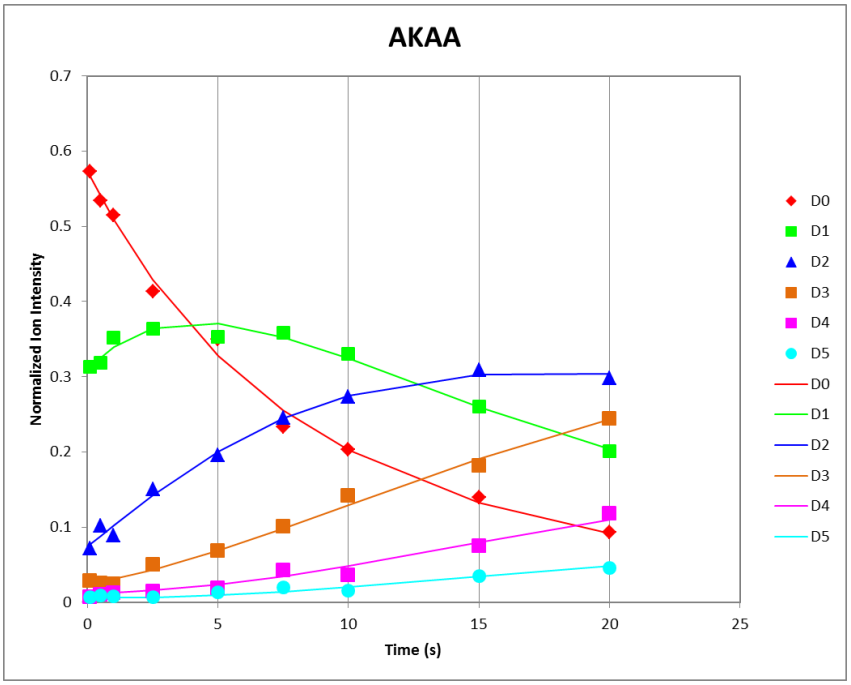
AKAA
Normalized Ion Intensity
Time (s)
0
0.1
0.2
0.3
0.4
0.5
0.6
0.7
0
5
10
15
20
25
D0
D1
D2
D3
D4
D5
D0
D1
D2
D3
D4
D5

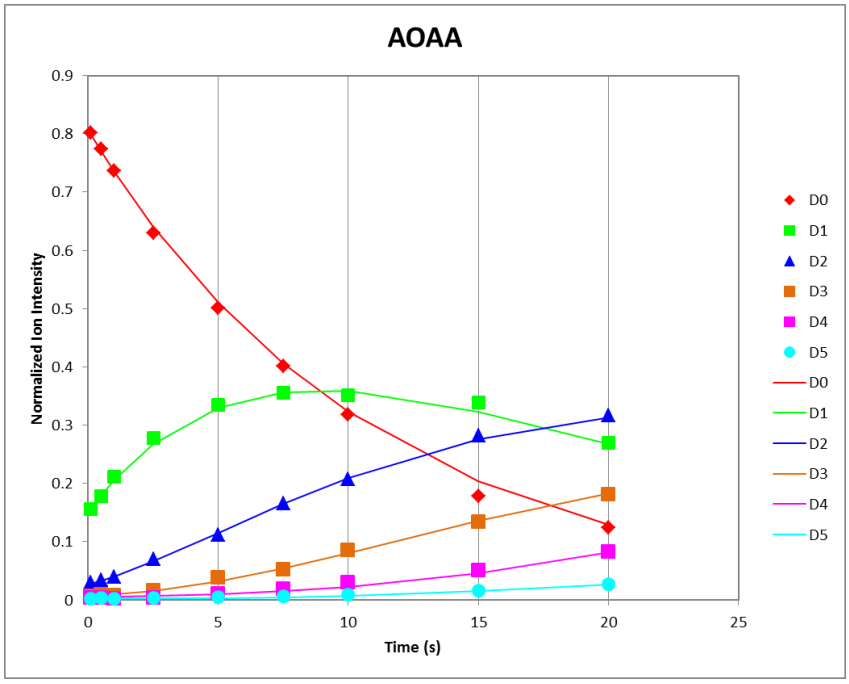
AOAA
Normalized Ion Intensity
Time (s)
0
0.1
0.2
0.3
0.4
0.5
0.6
0.7
0.8
0.9
0
5
10
15
20
25
D0
D1
D2
D3
D4
D5
D0
D1
D2
D3
D4
D5

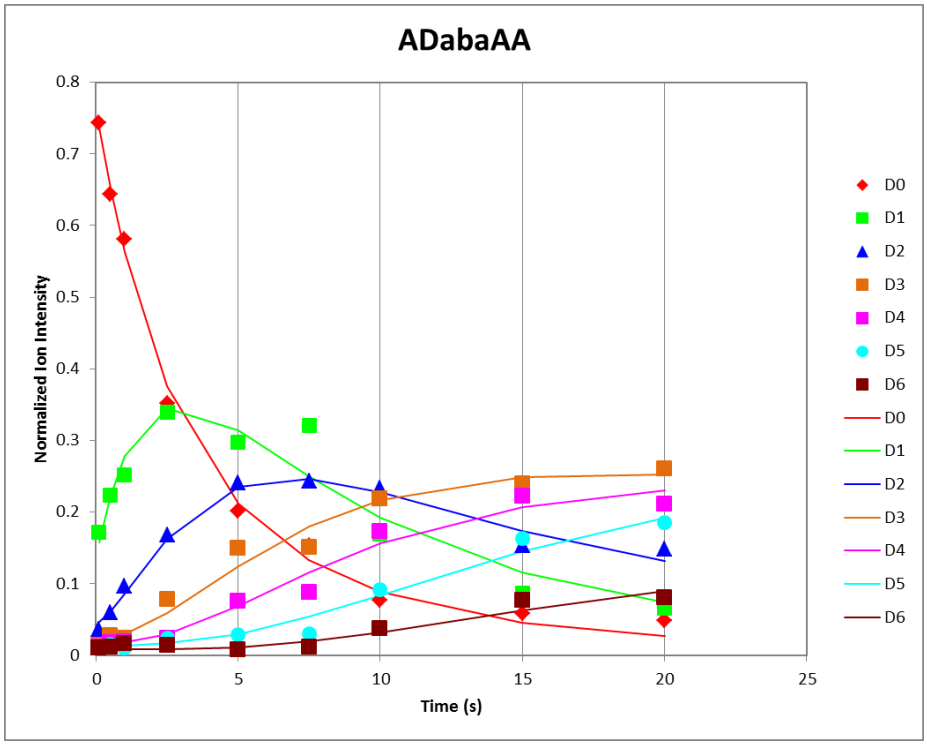
ADabaAA
Normalized Ion Intensity
Time (s)
0
0.1
0.2
0.3
0.4
0.5
0.6
0.7
0.8
0
5
10
15
20
25
D0
D1
D2
D3
D4
D5
D6
D0
D1
D2
D3
D4
D5
D6

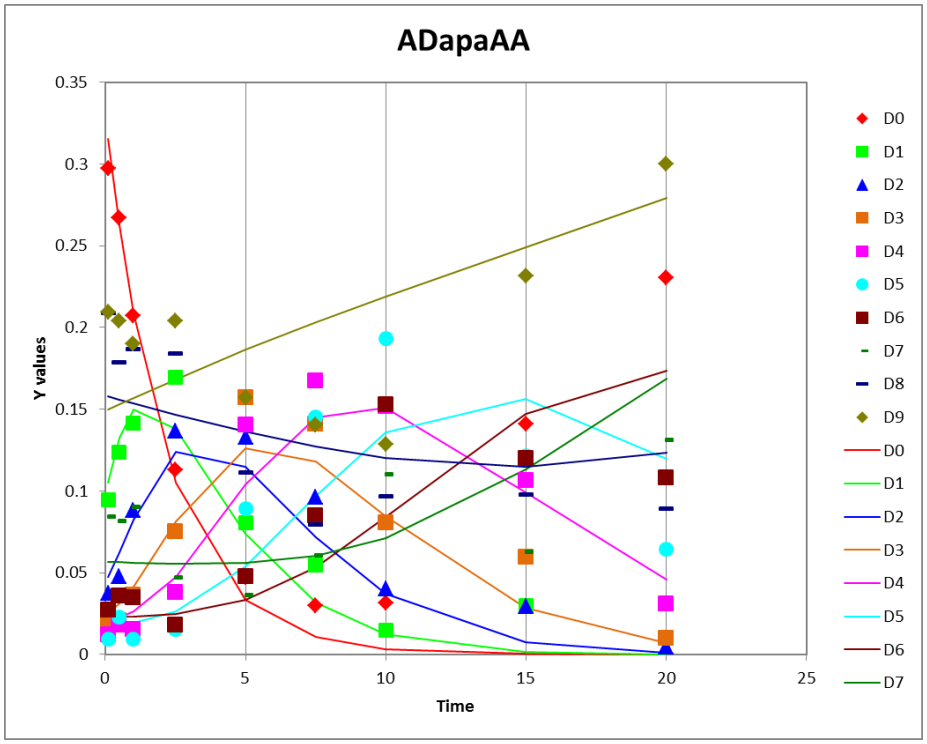
ADapaAA
Y values
Time
0
0.05
0.1
0.15
0.2
0.25
0.3
0.35
0
5
10
15
20
25
D0
D1
D2
D3
D4
D5
D6
D7
D8
D9
D0
D1
D2
D3
D4
D5
D6
D7

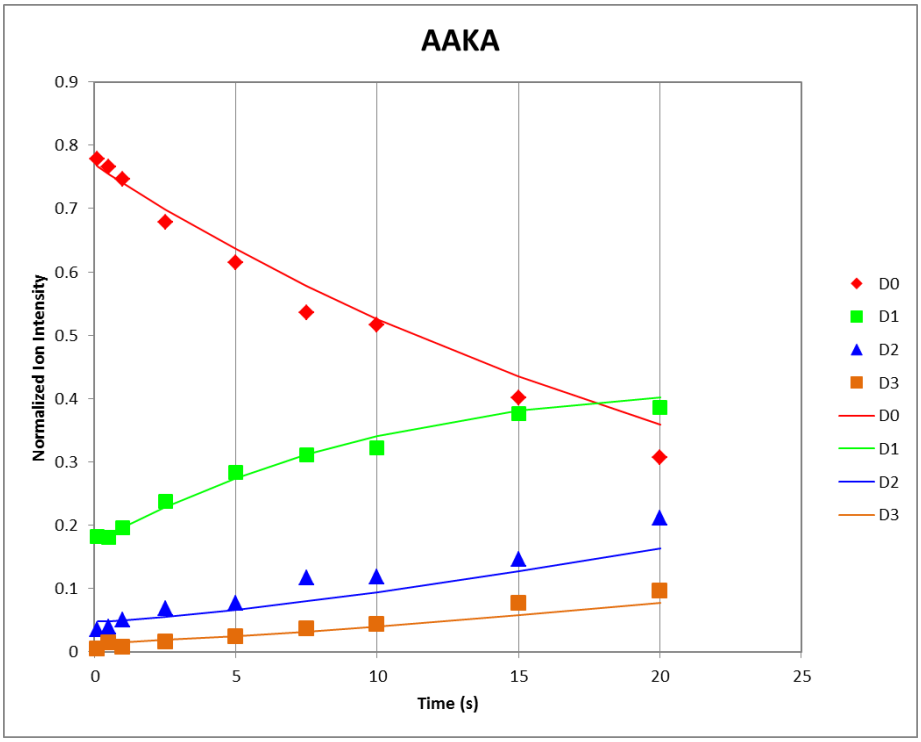
AAKA
Normalized Ion Intensity
Time (s)
0
0.1
0.2
0.3
0.4
0.5
0.6
0.7
0.8
0.9
0
5
10
15
20
25
D0
D1
D2
D3
D0
D1
D2
D3

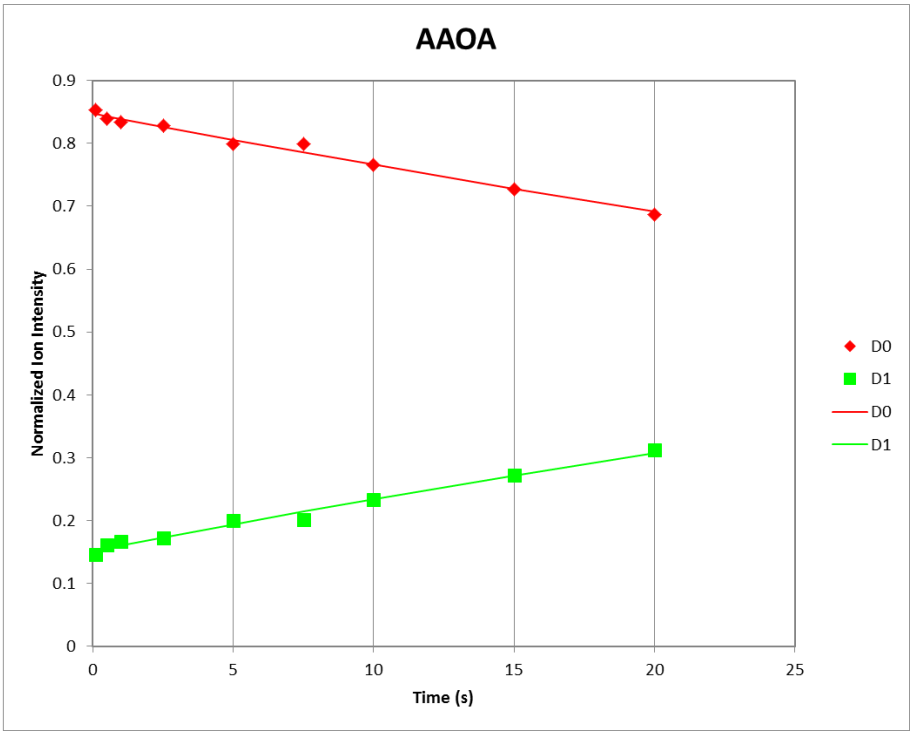
AAOA
Normalized Ion Intensity
Time (s)
0
0.1
0.2
0.3
0.4
0.5
0.6
0.7
0.8
0.9
0
5
10
15
20
25
D0
D1
D0
D1

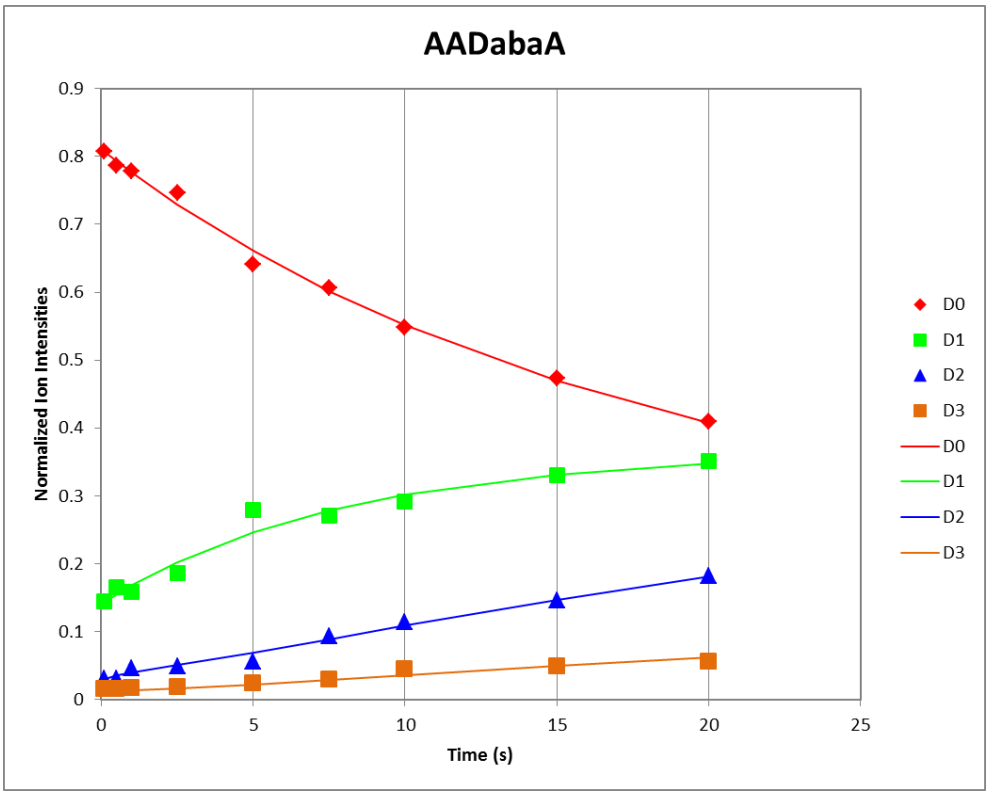
AADabaA
Normalized Ion Intensities
Time (s)
0
0.1
0.2
0.3
0.4
0.5
0.6
0.7
0.8
0.9
0
5
10
15
20
25
D0
D1
D2
D3
D0
D1
D2
D3

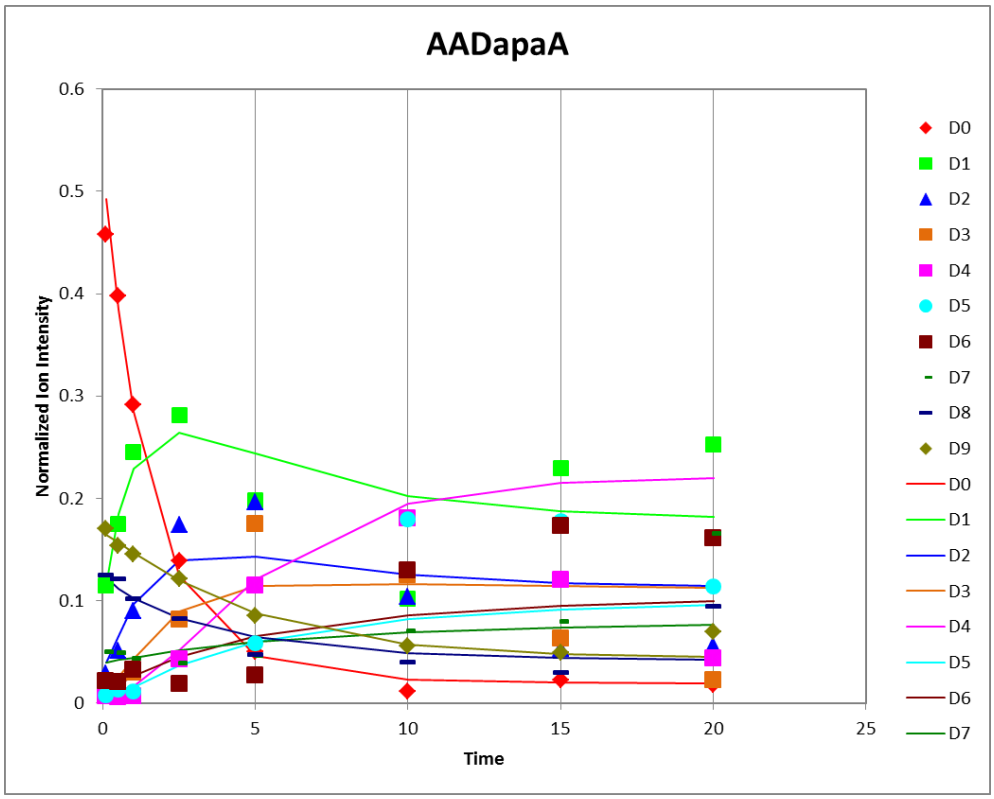
AADapaA
Normalized Ion Intensity
Time
0
0.1
0.2
0.3
0.4
0.5
0.6
0
5
10
15
20
25
D0
D1
D2
D3
D4
D5
D6
D7
D8
D9
D0
D1
D2
D3
D4
D5
D6
D7

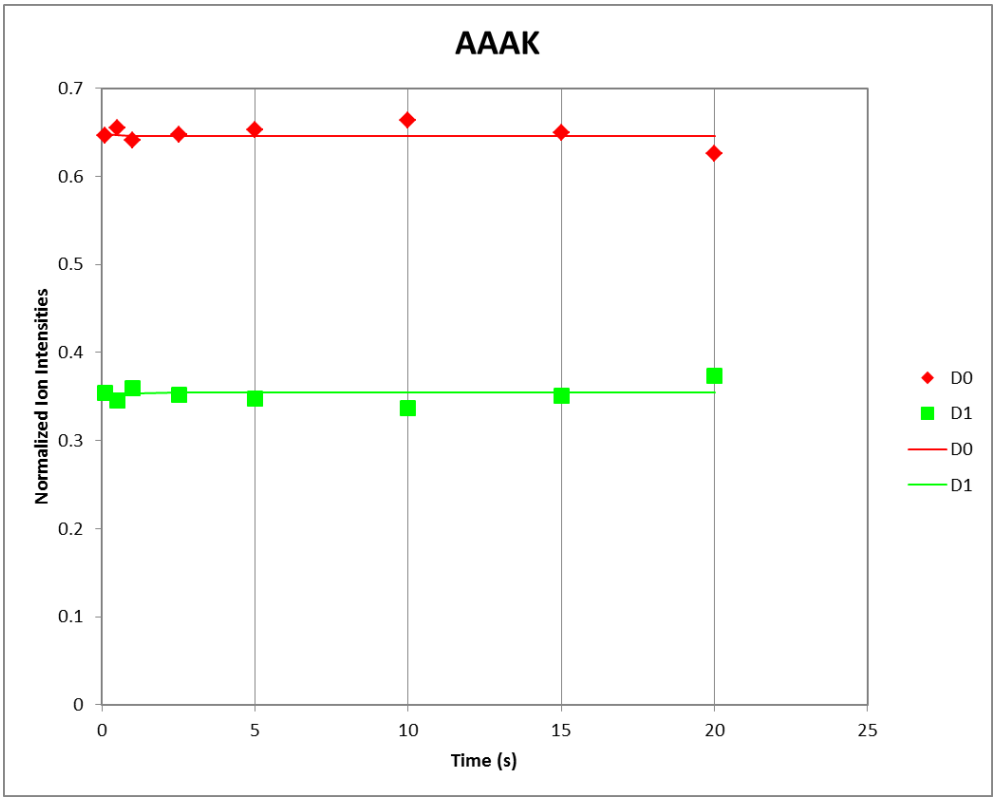
AAAK
Normalized Ion Intensities
0.7
0.6
0.5
0.4
0.3
0.2
0.1
0
0
5
10
15
20
25
Time (s)
D0
D1
D0
D1

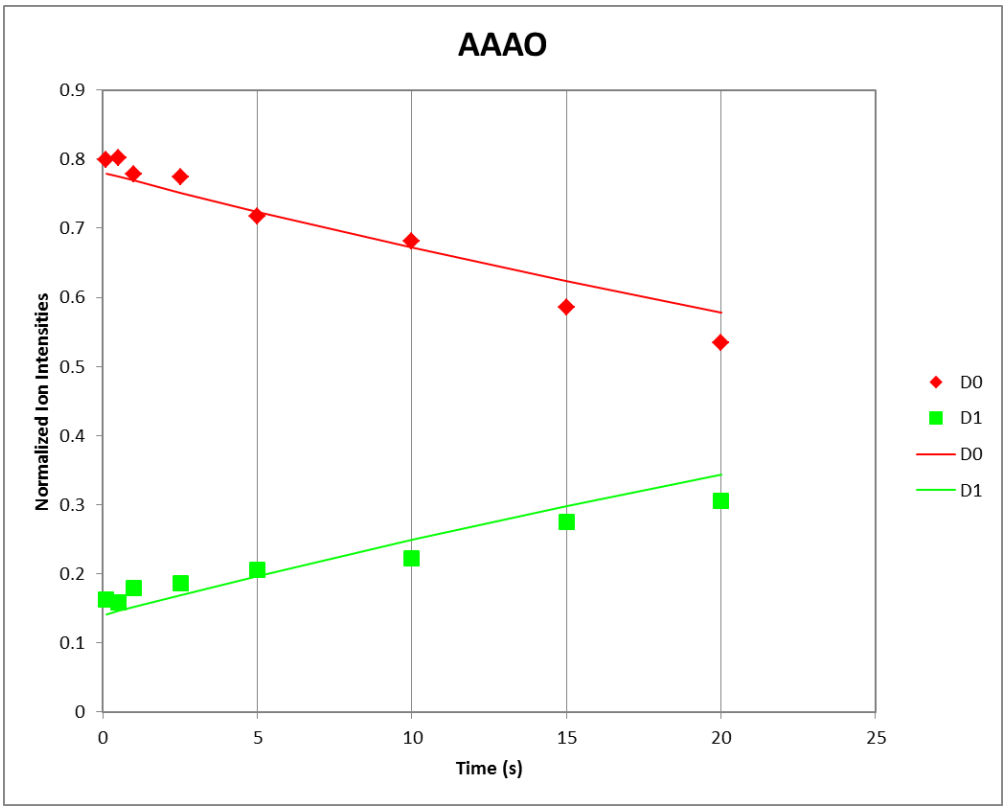
AAAO
Normalized Ion Intensities
0.9
0.8
0.7
0.6
0.5
0.4
0.3
0.2
0.1
0
0
5
10
15
20
25
Time (s)
D0
D1
D0
D1

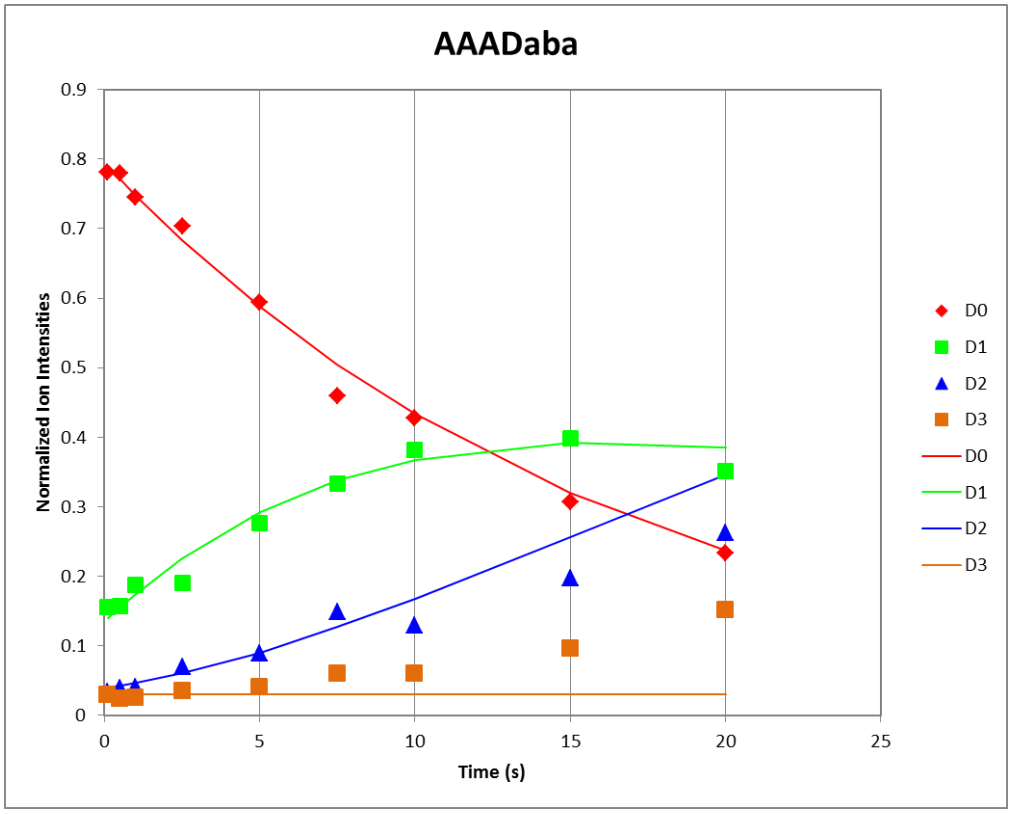
AAADaba
Normalized Ion Intensities
Time (s)
0
0.1
0.2
0.3
0.4
0.5
0.6
0.7
0.8
0.9
0
5
10
15
20
25
D0
D1
D2
D3
D0
D1
D2
D3

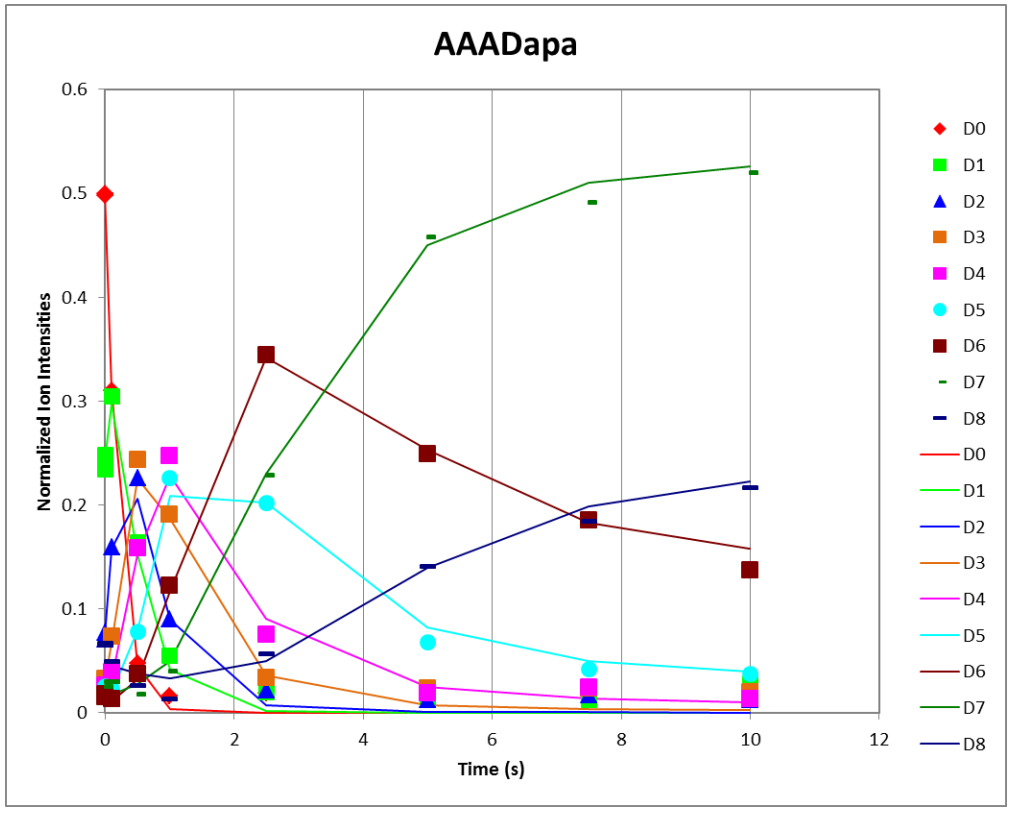
AAADapa
Normalized Ion Intensities
Time (s)
0
0.1
0.2
0.3
0.4
0.5
0.6
0
2
4
6
8
10
12
D0
D1
D2
D3
D4
D5
D6
D7
D8
D0
D1
D2
D3
D4
D5
D6
D7
D8

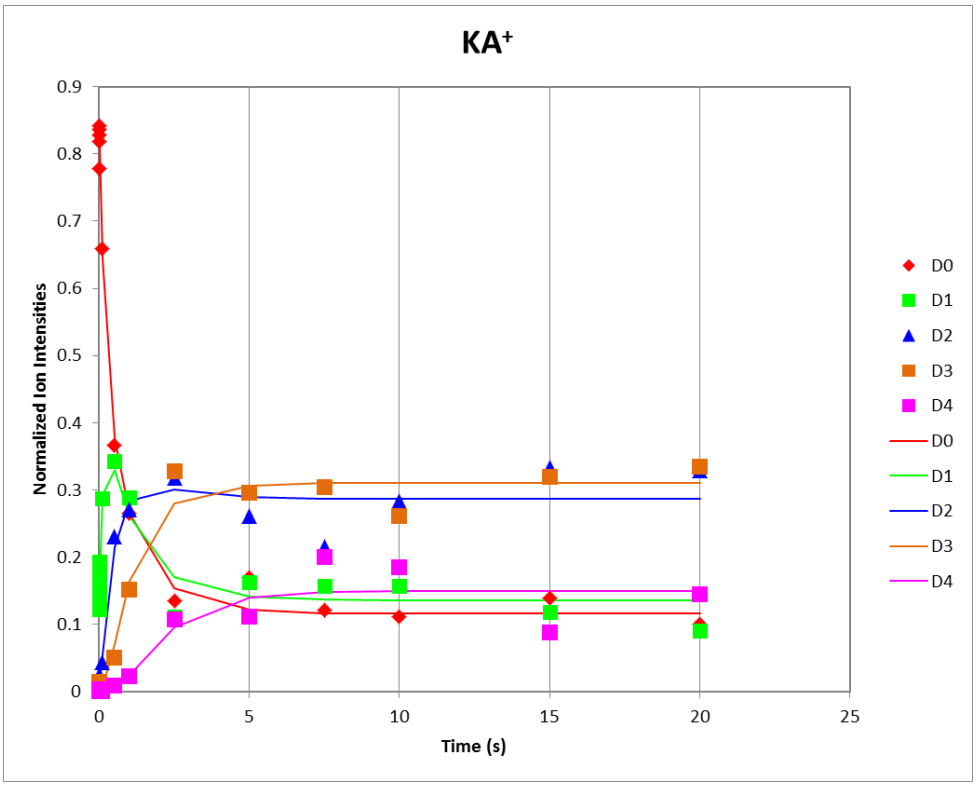
KA+
Normalized Ion Intensities
Time (s)
0
0.1
0.2
0.3
0.4
0.5
0.6
0.7
0.8
0.9
0
5
10
15
20
25
D0
D1
D2
D3
D4
D0
D1
D2
D3
D4

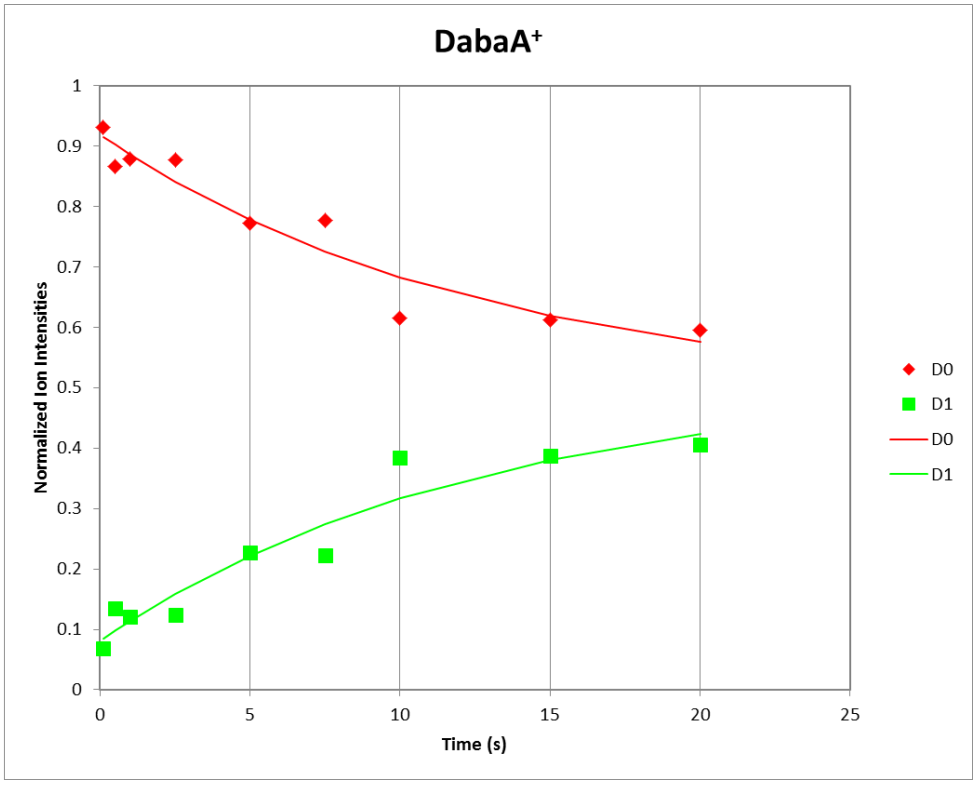
DabaA+
Normalized Ion Intensities
Time (s)
0
0.1
0.2
0.3
0.4
0.5
0.6
0.7
0.8
0.9
1
0
5
10
15
20
25
D0
D1
D0
D1

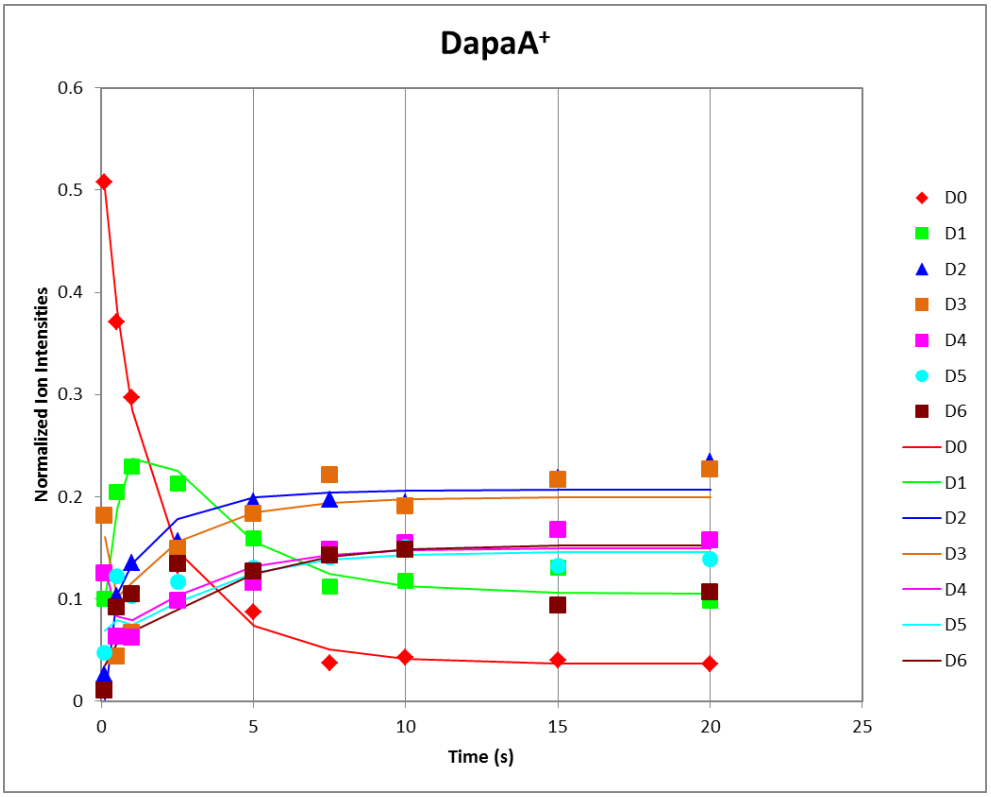
DapaA+
Normalized Ion Intensities
Time (s)
0
0.1
0.2
0.3
0.4
0.5
0.6
0
5
10
15
20
25
D0
D1
D2
D3
D4
D5
D6
D0
D1
D2
D3
D4
D5
D6

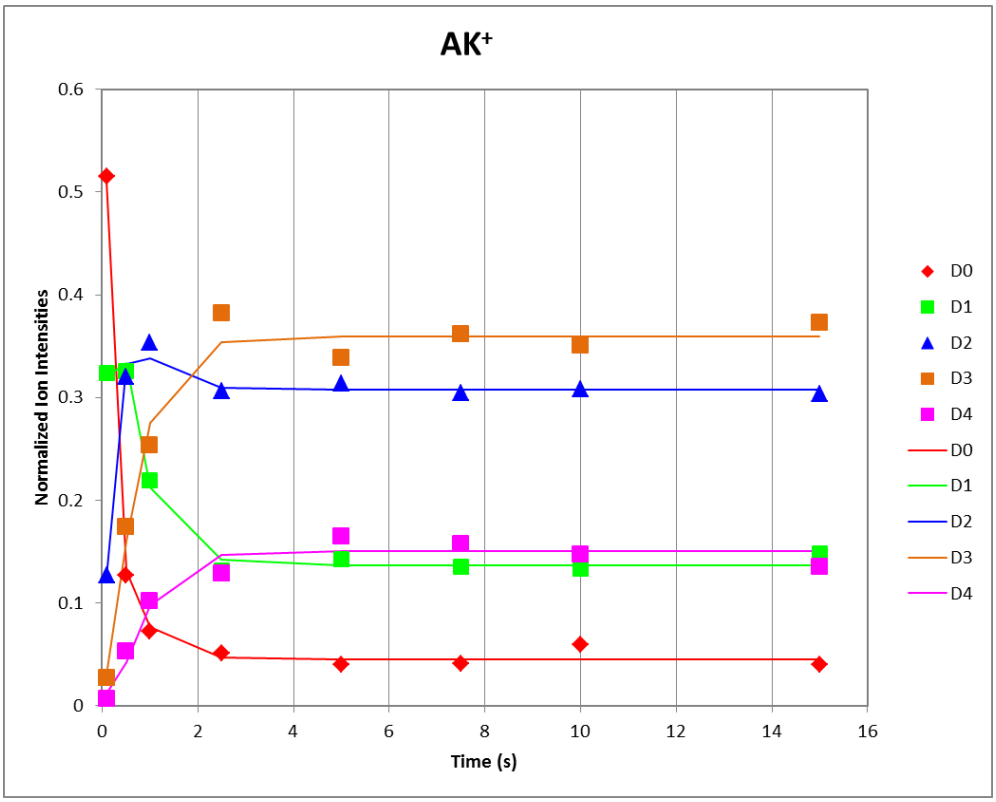
AK+
Normalized Ion Intensities
Time (s)
0
0.1
0.2
0.3
0.4
0.5
0.6
0
2
4
6
8
10
12
14
16
D0
D1
D2
D3
D4
D0
D1
D2
D3
D4

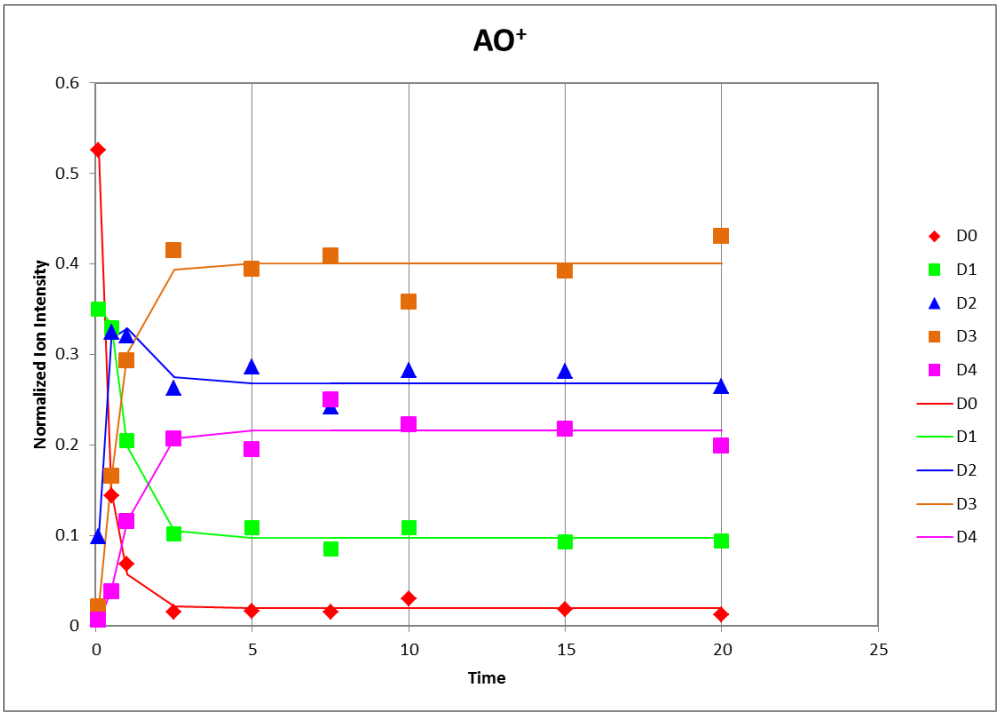
AO+
Normalized Ion Intensity
Time
0.6
0.5
0.4
0.3
0.2
0.1
0
0
5
10
15
20
25
D0
D1
D2
D3
D4
D0
D1
D2
D3
D4

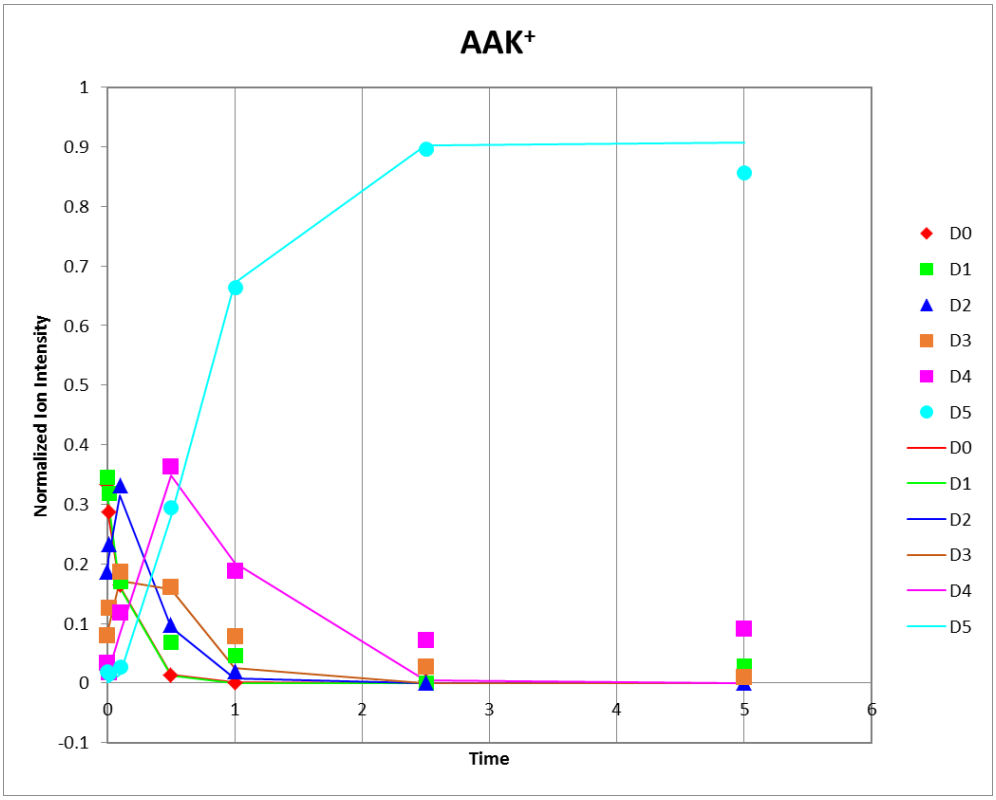
AAK+
Normalized Ion Intensity
Time
1
0.9
0.8
0.7
0.6
0.5
0.4
0.3
0.2
0.1
0
-0.1
0
1
2
3
4
5
6
D0
D1
D2
D3
D4
D5
D0
D1
D2
D3
D4
D5

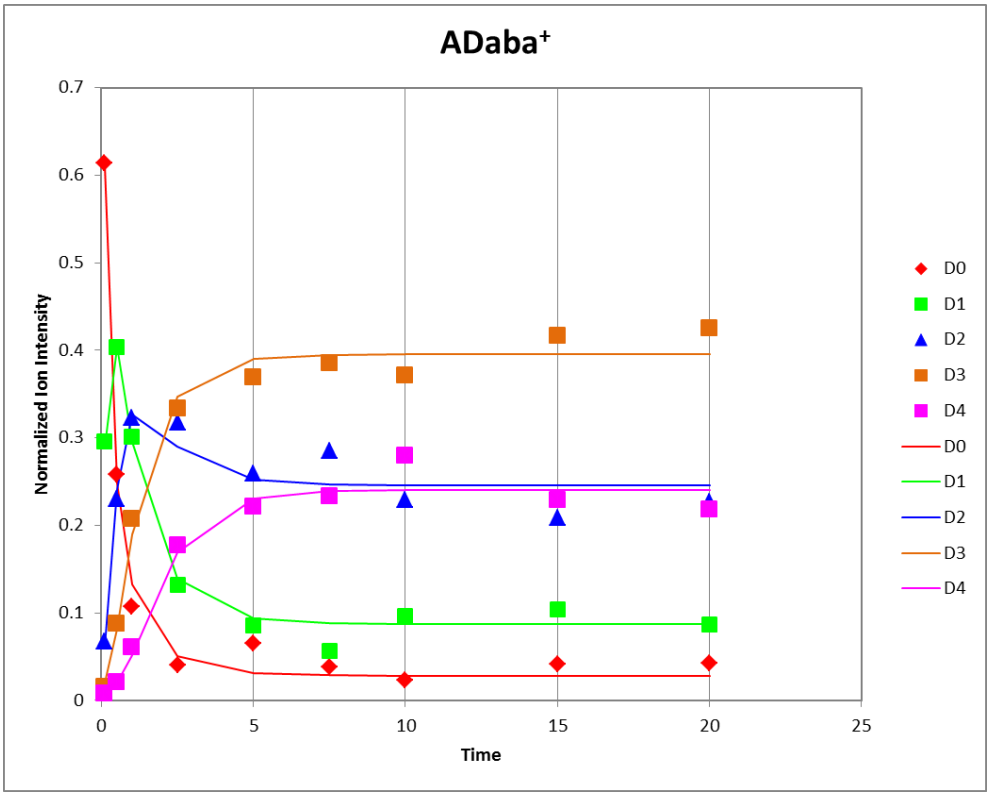
ADaba+
Normalized Ion Intensity
Time
0
0.1
0.2
0.3
0.4
0.5
0.6
0.7
0
5
10
15
20
25
D0
D1
D2
D3
D4
D0
D1
D2
D3
D4

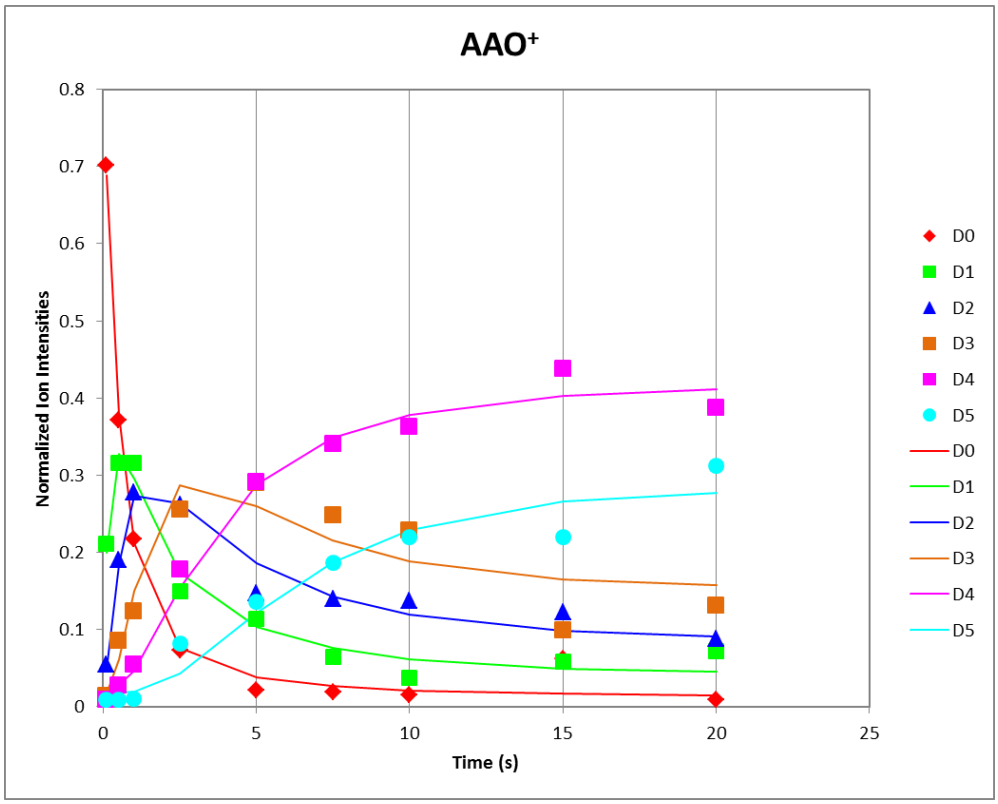
AAO+
Normalized Ion Intensities
Time (s)
0
0.1
0.2
0.3
0.4
0.5
0.6
0.7
0.8
0
5
10
15
20
25
D0
D1
D2
D3
D4
D5
D0
D1
D2
D3
D4
D5

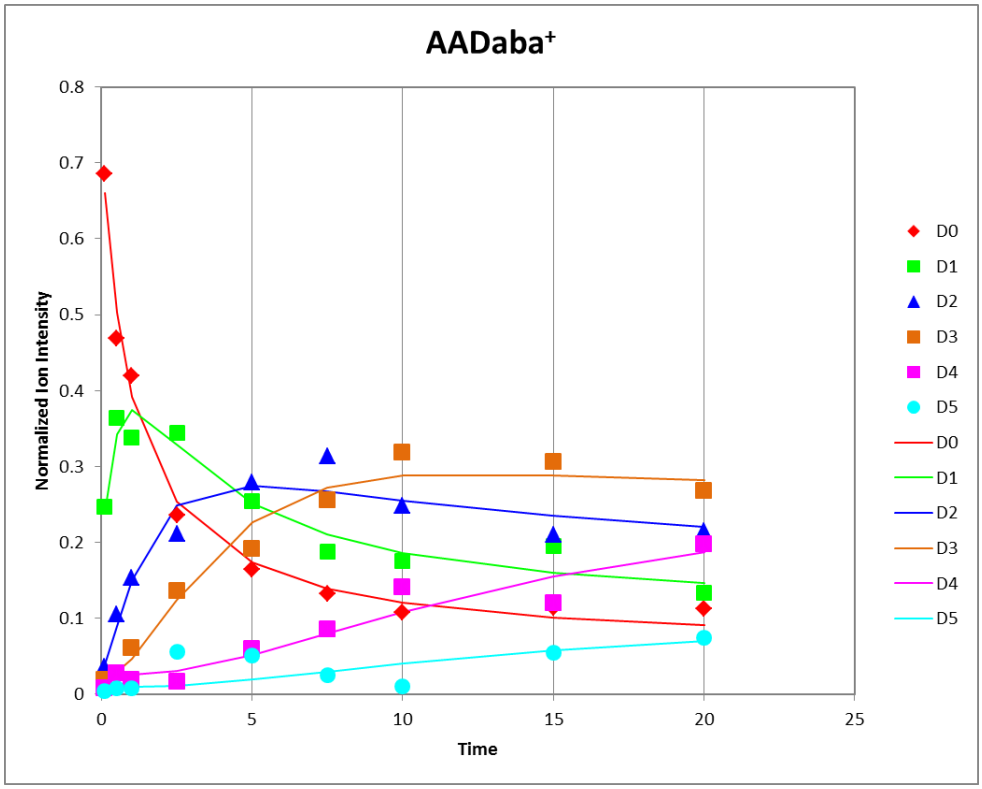
AADaba+
Normalized Ion Intensity
Time
0
0.1
0.2
0.3
0.4
0.5
0.6
0.7
0.8
0
5
10
15
20
25
D0
D1
D2
D3
D4
D5
D0
D1
D2
D3
D4
D5

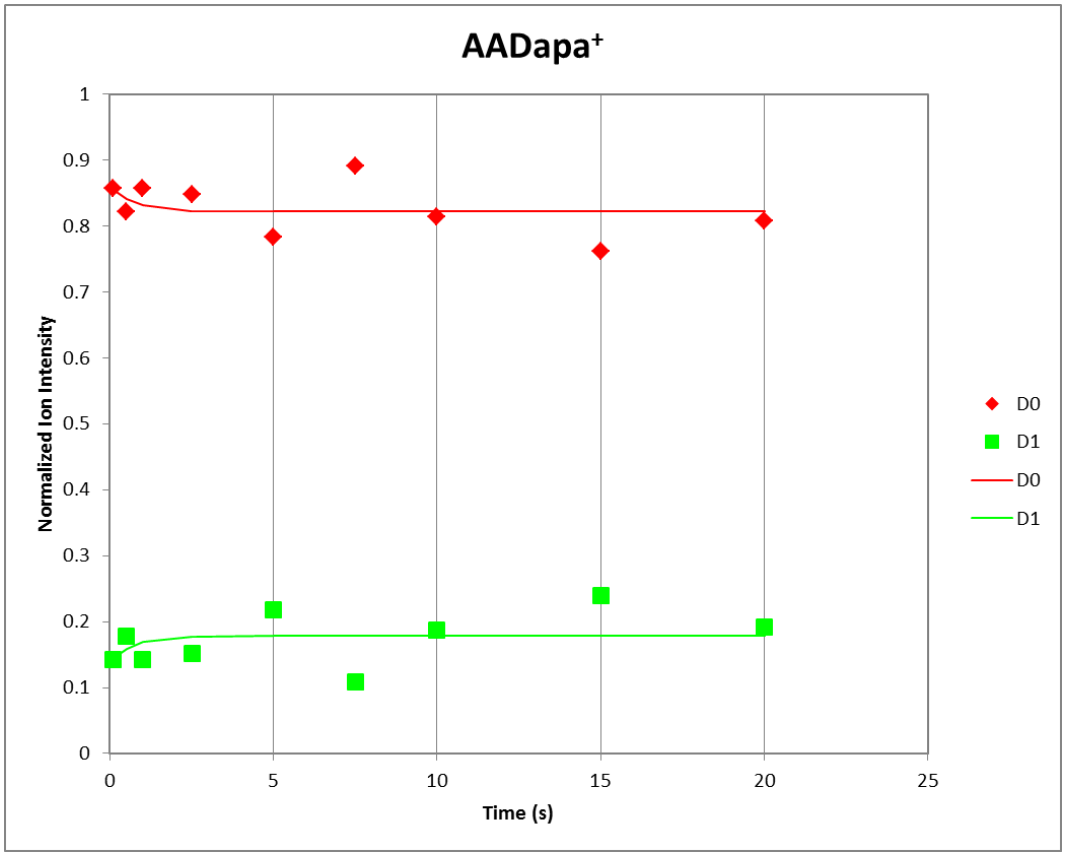
AADapa+
Normalized Ion Intensity
Time (s)
0
0.1
0.2
0.3
0.4
0.5
0.6
0.7
0.8
0.9
1
0
5
10
15
20
25
D0
D1
D0
D1